ARMY RESEARCH LABORATORY

ARL

The Particulation of a Shaped Charge Jet for Face-Centered-Cubic Liner Materials

William P. Walters
Richard L. Summers

ARL-TR-114 April 1993

NOTICES

Destroy this report when it is no longer needed. DO NOT return it to the originator.

Additional copies of this report may be obtained from the National Technical Information Service, U.S. Department of Commerce, 5285 Port Royal Road, Springfield, VA 22161.

The findings of this report are not to be construed as an official Department of the Army position, unless so designated by other authorized documents.

The use of trade names or manufacturers' names in this report does not constitute indorsement of any commercial product.

REPORT DOCUMENTATION PAGE

Form Approved
OMB No. 0704-0188

1. AGENCY USE ONLY (Leave blank)	2. REPORT DATE	3. REPORT TYPE AND DATES COVERED
	April 1993	Final, January 1992–January 1993

4. TITLE AND SUBTITLE

The Particulation of a Shaped Charge Jet for Face-Centered-Cubic Liner Materials

5. FUNDING NUMBERS

PR: 1L162618AH80

6. AUTHOR(S)

William P. Walters and Richard L. Summers

7. PERFORMING ORGANIZATION NAME(S) AND ADDRESS(ES)

U.S. Army Research Laboratory
ATTN: AMSRL-WT-TC
Aberdeen Proving Ground, MD 21005-5066

8. PERFORMING ORGANIZATION REPORT NUMBER

9. SPONSORING/MONITORING AGENCY NAME(S) AND ADDRESS(ES)

U.S. Army Research Laboratory
ATTN: AMSRL-OP-CI-B (Tech Lib)
Aberdeen Proving Ground, MD 21005-5066

10. SPONSORING/MONITORING AGENCY REPORT NUMBER

ARL-TR-114

11. SUPPLEMENTARY NOTES

12a. DISTRIBUTION/AVAILABILITY STATEMENT

Approved for public release; distribution is unlimited.

12b. DISTRIBUTION CODE

13. ABSTRACT (Maximum 200 words)

An analytical model was derived to predict the breakup time distribution and the strain at breakup of the jet from a shaped charge liner. The model invoked a plastic stability criterion, kinematic considerations, and the Zerilli-Armstrong constitutive model for face-centered-cubic liner materials. The model revealed excellent agreement with experimental data for several liner geometries but is strongly dependent on the jet temperature distribution as well as the initial strain rate.

14. SUBJECT TERMS

strain rate, kinematics, velocity, cumulative breakup time, particulation

15. NUMBER OF PAGES

51

16. PRICE CODE

17. SECURITY CLASSIFICATION OF REPORT	18. SECURITY CLASSIFICATION OF THIS PAGE	19. SECURITY CLASSIFICATION OF ABSTRACT	20. LIMITATION OF ABSTRACT
UNCLASSIFIED	UNCLASSIFIED	UNCLASSIFIED	UL

INTENTIONALLY LEFT BLANK.

PREFACE

On 30 September 1992, the U.S. Army Ballistic Research Laboratory (BRL) was deactivated and subsequently became part of the U.S. Army Research Laboratory (ARL) on 1 October 1992.

INTENTIONALLY LEFT BLANK.

TABLE OF CONTENTS

INTENTIONALLY LEFT BLANK.

LIST OF FIGURES

1. INTRODUCTION

A cylinder of explosive with a hollow cavity in one end and a detonator at the opposite end is known as a shaped charge. The hollow cavity (which may assume almost any geometric shape such as a hemisphere, cone, tulip, trumpet, or, in fact, any arcuate device) is usually lined with a thin layer of metal. The liner forms a jet when the explosive charge is detonated. Upon detonation, a spherical wave propagates outward from the point of initiation. This high-pressure shock wave moves at a very high velocity, typically around 10 km/s. As the detonation wave engulfs the lined cavity, the material is accelerated under the high detonation pressure, collapsing the liner. During this process the liner material is driven to very violent distortions over very short time intervals, at strain rates of 10^4 to 10^7 s^{-1} and peak strains greater than 10 are possible. The jet temperature is about 500 to 900 K according to the measurements of von Holle and Trimble and there may be temperature gradients along and through the jet. The collapse of the conical liner material onto the centerline forces a portion of the liner to flow in the form of a jet where the jet tip can travel in excess of 10 km/s. Because of the presence of an axial velocity gradient, the jet will stretch until it fractures into a column of particles. This fracture of the jet into a series of particles is termed jet breakup or particulation.

The penetration of a shaped charge jet into most target materials increases to a maximum and then decreases as the standoff distance (distance from the front of the shaped charge to the target) increases. This penetration peak occurs just prior to the onset of jet breakup due to the dispersion, spread, and tumbling of the jet particles after particulation. As a result, it would be advantageous to the shaped charge designer to predict and control the jet breakup time.

The nature of the particulation of the shaped charge jet has been of interest for over 50 years. It is known that some materials, namely, certain metals, exhibit extreme ductility under the intense dynamic conditions involved in the shaped charge collapse process. These materials often do not possess the same degree of ductility under ambient conditions and undergo dynamic elongations of 1,000% or more. The problem is complicated by the fact that the material properties of the liner are not well known under the intense dynamic conditions that the jet undergoes during its collapse, formation, and growth. Complex hydrocode computer programs are limited because accurate equations of state and constitutive equations are not available under these conditions. Also, the fracture mechanism and associated algorithm is not well known. Nevertheless, shaped charge experiments provide an excellent test bed for the study of materials under intense loading conditions.

2. EXPERIMENTAL APPROACH

The experimental characterization of shaped charge jets is most commonly performed using multiple flash x-ray units. Each flash x-ray unit provides an image of the shaped charge jet at a known time. In a typical experiment, several x-ray units are flashed at pre-determined time intervals. The x-ray films are then analyzed to determine the position, length, radius, mass, and velocity of each of the jet particles. In general, the entire shaped charge jet cannot be captured in a single experiment due to limitations in the length of x-ray film which can be exposed and the need to protect the film from the explosive blast. The data obtained from the x-ray films is utilized to calculate the jet breakup time.

The jet breakup time can be experimentally determined in several ways with varying results. The most common method of calculating an aggregate jet breakup time is to divide the cumulative jet length by the change in the jet velocity from the tip particle to the slowest jet particle characterized in the experiment. This "slowest" particle may or may not be the rear of the jet. This method provides a single value, termed the "cumulative breakup time," for the entire jet. The cumulative breakup time is based on several assumptions. The jet is assumed to stretch from an initial length of zero at a constant, uniform rate. In addition, the jet is assumed to break simultaneously, from tip to tail, at the time it reaches its maximum length.

The cumulative breakup time provides an accurate measure of the total jet length available for penetration if it is observed that the cumulative jet length is a linear function of the velocity of the jet particles. However, in many cases, the cumulative jet length is nonlinear with respect to the jet velocity. In such cases, the value of the cumulative breakup time will vary with the velocity of the slowest jet particle included in the calculation. For example, Figure 1 is a plot of the cumulative breakup time as a function of the velocity of the slowest jet particle included in the calculation. This plot was derived from a single experiment involving the Ballistic Research Laboratory (BRL) 81-mm standard shaped charge. The velocity of the tip particle was 7.7 km/s, and the velocity of the slowest particle characterized in the experiment was 2.1 km/s. The cumulative breakup time for this experiment was found to be 147.8 μs. The data plotted were determined as the sum of the lengths of the first n particles divided by the velocity difference between the first particle and the n^{th} particle. The axial velocity in Figure 1 reflects the velocity of the n^{th} particle. The extremely large breakup times observed in the leading portion of the jet are due in part to the deceleration of the tip particle which reduces the difference in velocity between the

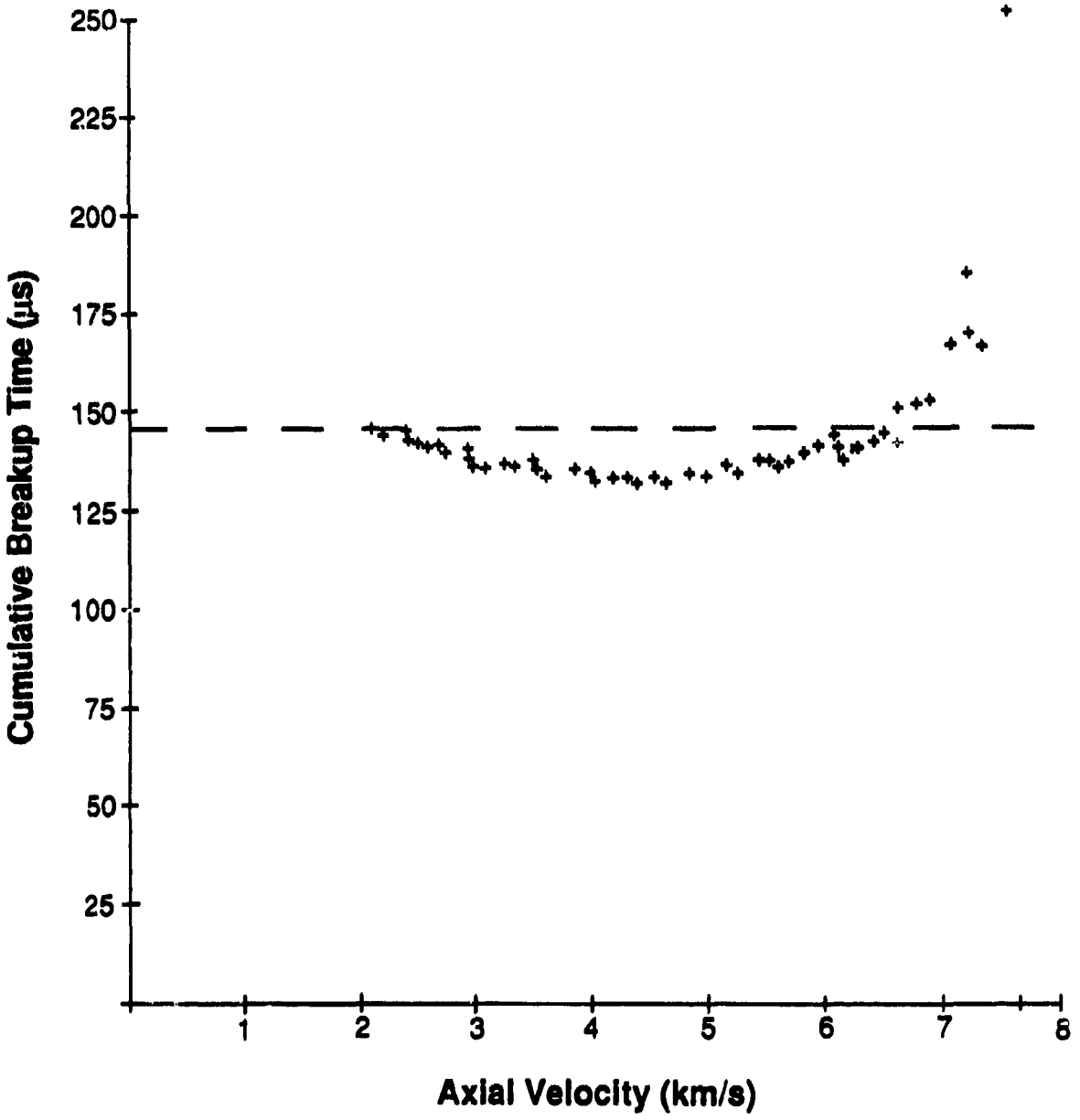

Figure 1. Cumulative breakup time vs. axial velocity.

tip particle and the particles immediately following. As evidenced in Figure 1, the measured value of the cumulative breakup time is dependent on the experimental setup. If, for example, the experimental setup were such that only the jet particles travelling faster than 4 km/s were characterized, then the cumulative breakup time would be reported as 132 μs.

A more accurate representation of the experimental data may be obtained by treating the cumulative jet length as a piecewise linear function of the jet velocity (Held 1985). Thus, the jet breakup time may be calculated for several velocity ranges. In fact, the breakup time can be calculated for each particle. For example, Figure 2 is a plot of the individual breakup times calculated for the same 81-mm standard shaped charge. The individual breakup time is extremely sensitive to nonuniform velocity differences between particles and to measurement error. Some of the jet particles separate from one another at breakup but travel at very nearly identical velocities after separation, thus allowing unrealistically large absolute values of breakup times to be computed. Breakup times which are calculated over large or predetermined velocity intervals are inherently more stable.

The breakup times, determined from analysis of the flash radiographs, discussed so far are based on the assumption that the jet stretches at a constant rate until it reaches a maximum length and particulates. The reference time for this process is the point in time and space from which the jet emanates, known as the "virtual origin." Conversely, the breakup time can also be calculated under the assumption that the jet particles travel at a constant velocity after the jet particulates. Thus, the time at which two jet particles separate from one another can be derived from the distance between the two particles at a known time and the velocity of the particles. The reference time in this case is determined by the experimentalist (i.e., the reference point may be the activation of the detonator, the time the detonation wave reaches the liner apex, the time the jet tip reaches the base of the liner, or other reference points). Figure 3 is a plot of the separation times computed from the 81-mm shaped charge experiment. The separation times plotted in Figure 3 are relative to the activation of the detonator. The separation times tend to increase with decreasing jet particle velocity, which indicates the jet broke from the tip to the tail, although in a nonuniform manner. The separation time calculation also tends to give unrealistic values when the difference in velocity between particles is nearly zero. However, unlike the individual breakup time calculation, the separation time is measured as a very small value (or large negative value) as the velocity difference approaches zero.

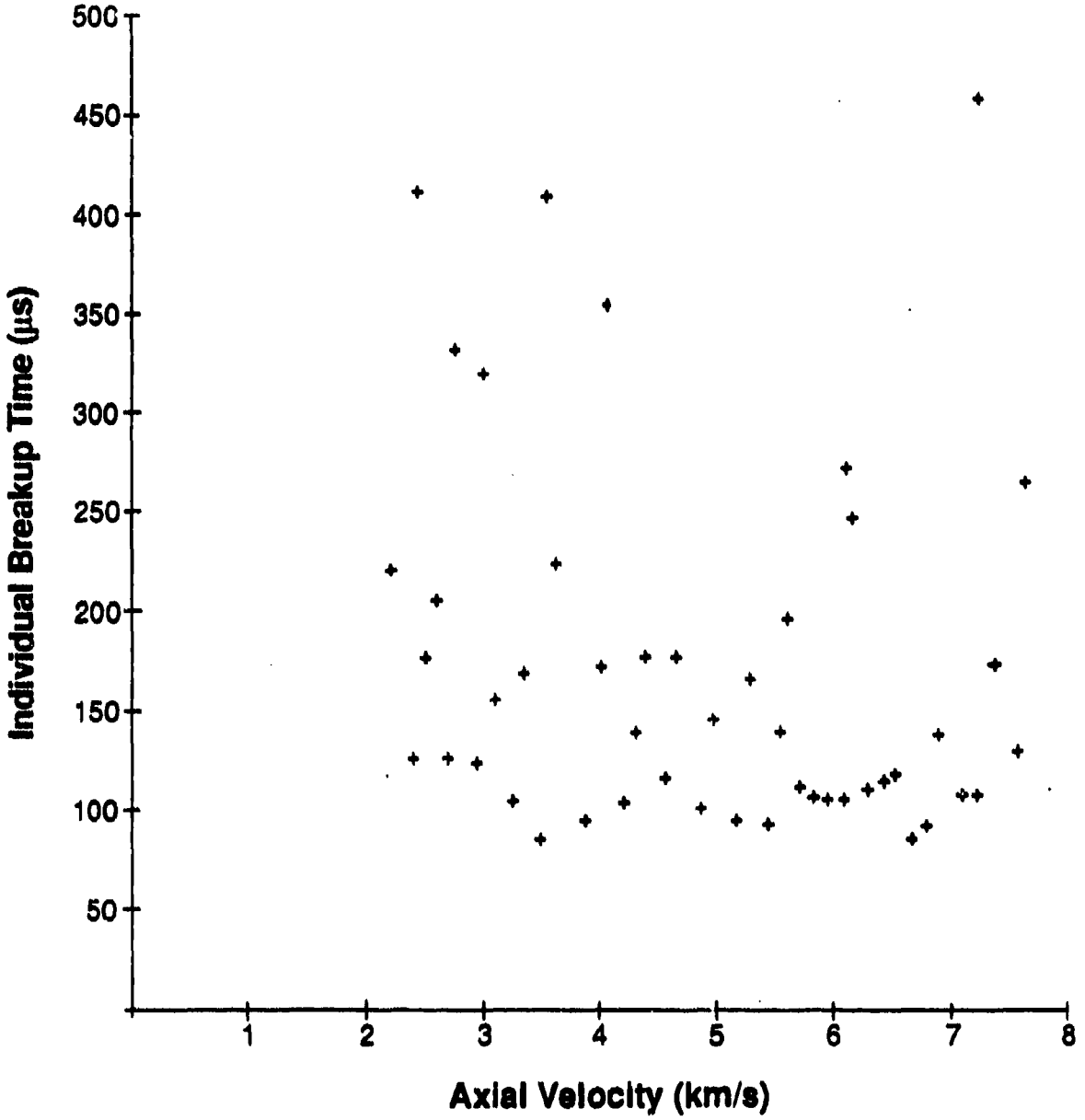

Figure 2. Individual breakup times vs. axial velocity.

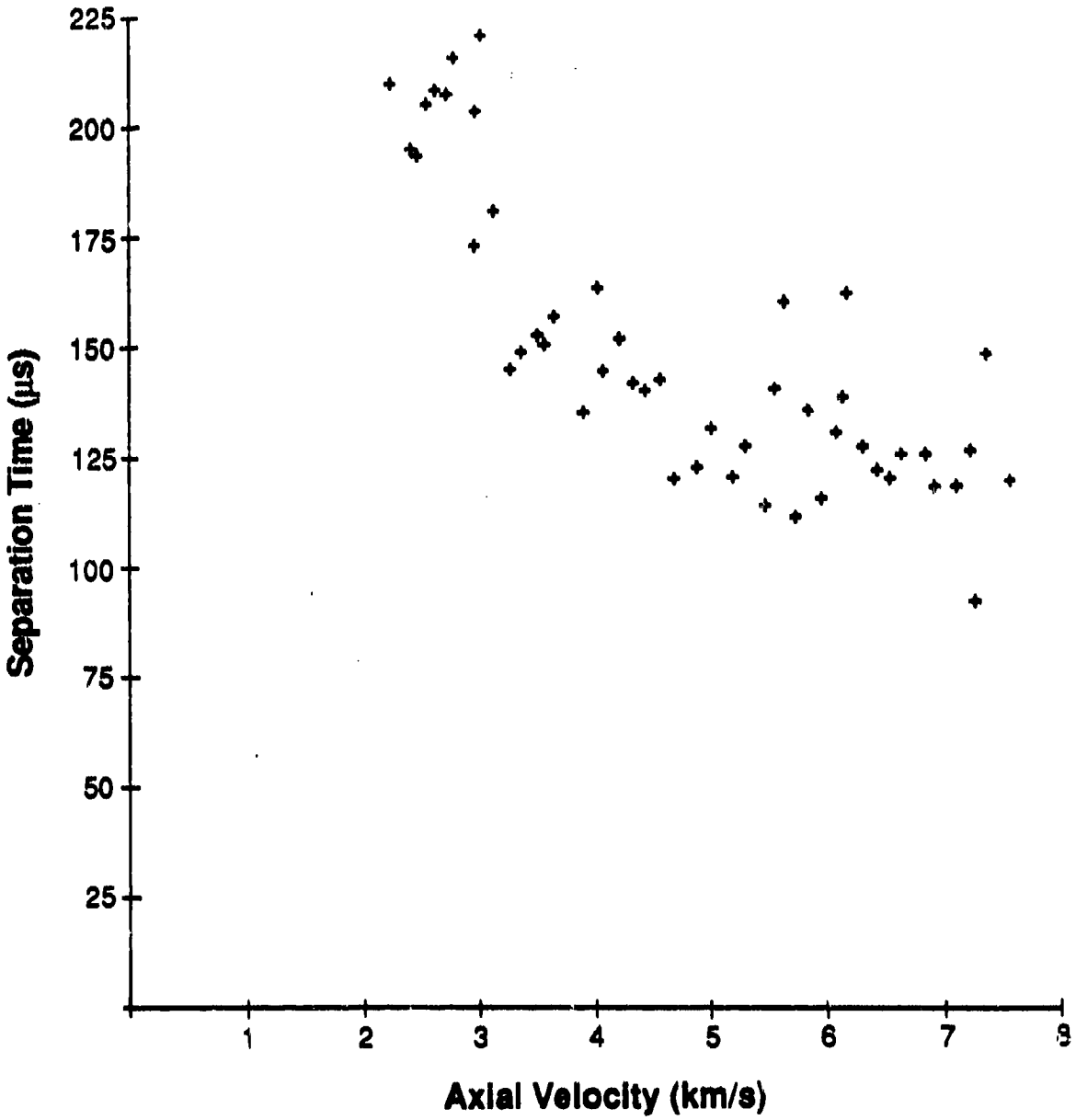

Figure 3. Separation times vs. axial velocity.

Also, the distance a jet particle travels before separation from its adjacent particles can be measured. The measurement of distance to particulation is very similar to the separation time measurement and is based on the same assumptions. Figure 4 is a plot of the separation distance vs. jet velocity again from the same 81-mm shaped charge experiment. The distance to separation is shown to decrease with decreasing jet velocity. The distance to separation is measured relative to the liner base.

3. ANALYTICAL MODELS: BACKGROUND

Analytical models of the jet breakup are available, notably due to Walsh, Held, Carleone, Chou, Pfeffer, Haugstad, and Hirsch, but are primarily one-dimensional and semi-empirical. More theoretical models are available from Pack, Curtis, Romero, Frankel, Weihs, and others. Early attempts at understanding the breakup of a shaped charge jet involved studies of liquid jet breakup since, visually, the breakup phenomenon would appear to have some analogy to the breakup of a liquid jet as studied by Rayleigh (1894). More recent liquid jet breakup studies concern atomization or the breakup of liquid drops in air where fluid viscosity and surface tension are the dominant mechanisms. Such analyses are given, for example, by Gordon (1959) and Heidmann and Groeneweg (1968). Tomotika (1935, 1936) considered the analysis of an incompressible, viscous Newtonian fluid surrounded by another viscous fluid under the action of capillary (viscous and surface tension) forces. A stability analysis was performed for the governing equations which accounted for stretching jets but neglected inertia effects. Mikami et al. (1974) studied the breakup of a viscous liquid thread in a viscous liquid (pulp fibers in water) for the paper pulp industry. Again, a stability analysis was performed for stretching jets in the absence of inertia terms. Goldin et al. (1969) considered the breakup of a viscoelastic fluid column, and extended the above analyses to a non-Newtonian flow. Frankel and Weihs (1985) attempted to directly consider the breakup of a shaped charge jet based on the studies described above but included inertial effects. The shaped charge jet was assumed to be liquid with a surface tension of 3×10^5 N/m. A perturbation solution was performed, but it was observed that the jet must have a very high yield strength (in excess of 2.4 GPa for copper) for the surface tension in the analysis to be meaningful. He noted that such high values of the dynamic yield strength of copper were quoted by Van Thiel and Levatin (1980). Curtis (1987) noted that the surface tension required to produce significant instability growth was of the order of the jet yield strength divided by the jet radius which is several orders of magnitude (namely, 4×10^5) greater than the known surface tension of copper in air at ambient conditions. Therefore, the tensile stress in the jet was considered to be the mechanism in the jet which produced the instability growth. Curtis used the equations of motion, the irrotationality condition, and the von Mises flow criterion, and he expressed the

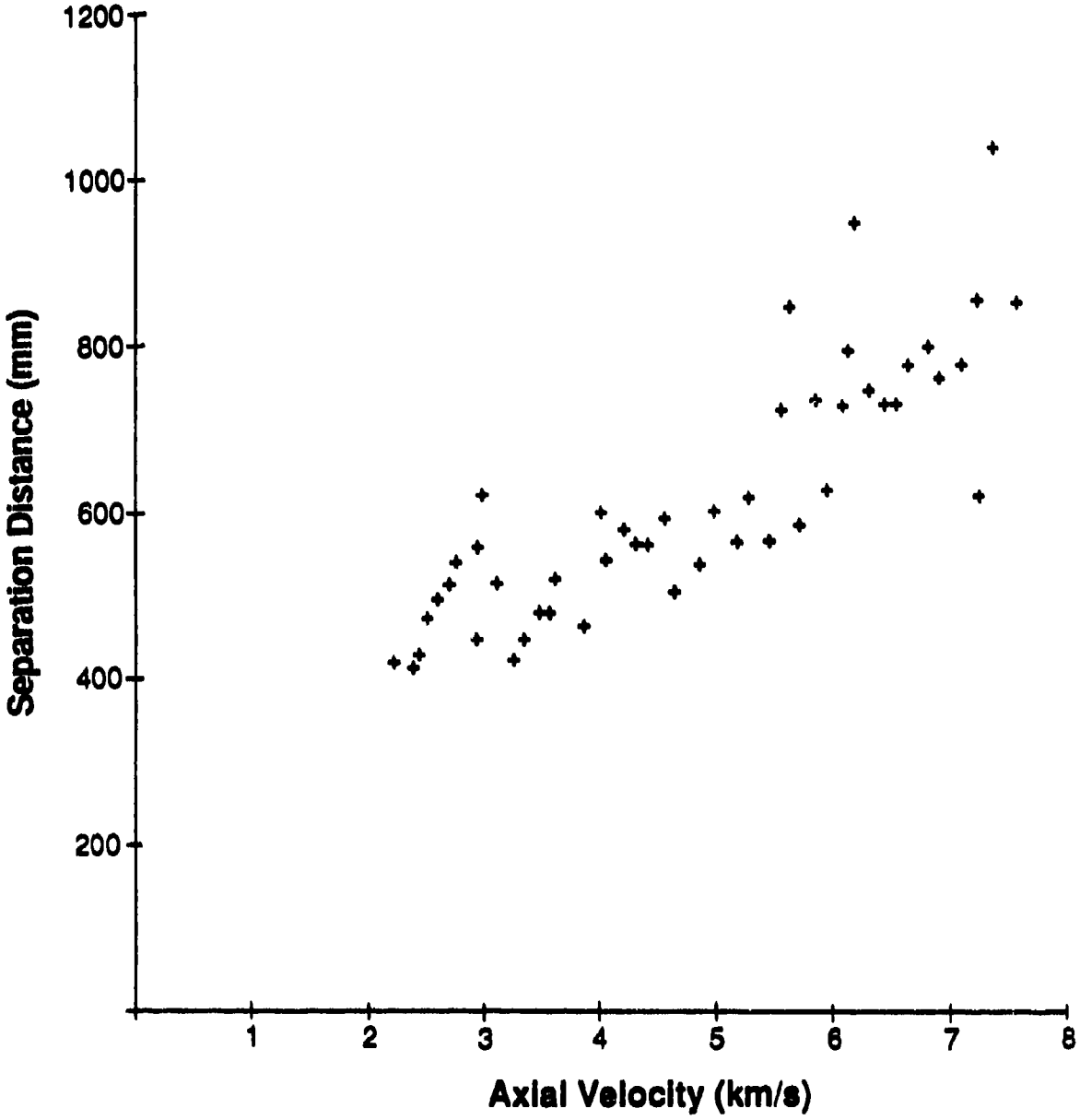

Figure 4. Distance to separation vs. axial velocity.

stress tensor as a superposition of a pressure term and a uniaxial stress term. A perturbation and stability analysis was performed for an assumed (zeroth order) velocity field. It was noted that the jet breakup is a function of the jet strength to density ratio, but the complexity of the equations precluded a detailed expression for the jet breakup time. Curtis concluded that it would be more appropriate to use the Levy-Mises flow criterion (the full classical plastic theory) instead of the von Mises criterion. Pack (1987) analyzed the plastic flow problem by using the equations of motion and the Levy-Mises stress-strain relationships plus the von Mises criterion for plastic flow. A perturbation analysis using a series solution was conducted along with a stability analysis, again for an assumed velocity field. Pack then postulated two causes of breakup: 1) necking of the jet, and 2) the creation of voids in the jet when all principal stresses become tensile. His predicted results for the two causes were very close and he was not able to distinguish between the two mechanisms. Romero (1989), along the same lines, performed a stability analysis of a rapidly stretching jet and concluded that the jet stability depends on a parameter he called "Γ," which represents the ratio of the inertial forces to the plastic forces. In fact, Γ is time dependent and

$$\Gamma^2(t) = \frac{\sqrt{3}}{\sigma}\rho\beta^2(t)a^2(t),$$

where a is the jet radius, β is the strain rate, ρ is the jet density, and σ is the yield stress. The jet is stable until Γ is less than 1. Romero's analysis was much like that of Frankel and Weih's, but used the Levy-Mises equations for a perfectly plastic material. As in the earlier analysis, a perturbation solution was obtained.

Other studies of the jet breakup time were conducted by Shelton and Arbuckle (1979) who considered the propagation of relief waves following a break in the jet. The speed of relief wave propagation from the break was calculated by two different models. Walsh (1984) provided insight into the mechanisms (i.e., surface disturbances) that may lead to jet instability. These disturbances include explosive homogeneity, liner dimensional tolerance, velocity gradient perturbations, and liner dynamic strength variations. Walsh concluded that breakup depends on the perturbation structure and a single dimensionless flow parameter,

$$\phi = \frac{\sigma/\rho}{\Delta V_0^2 R},$$

where σ is the yield strength of the jet, ρ is its density, R is the jet radius, and ΔV_o^2 is the initial jet stretch rate. The subscript o represents initial jet conditions. Finally, it was shown that the length traveled until breakup occurred, L_b, is given by

$$L_b = f(L_o, \phi_o, \Psi_o),$$

where L_o is the initial jet length, ϕ_o is the initial value of ϕ, and Ψ_o is the initial surface roughness.

Analytical, one-dimensional models are also available. Miller (1982) showed that a one-dimensional theory applied to a perfectly plastic stretching metal rod, or applied to a stretching metal rod governed by the Steinberg-Guinan-Cochran constitutive model, predicts the generation of a progression of new necks from an existing neck. Two-dimensional finite-difference calculations predict the same behavior.

Chou, Sidhi, and Mortimer (1963), in perhaps one of the earliest analytical studies of shaped charge jet breakup, deduced three possible mechanisms, or model approaches, for breakup. These mechanisms were viscoplastic effects (which as Chou et al. noted, would preclude Hopkinson scaling of the jet breakup—if this is a limitation); a Mott-type statistical approach which assumes that the tensile strength is not constant but exhibits a scatter characteristic (i.e., there exists a scatter in the value of the reduction in area (or value of strain) at which fracture occurs in a tensile test); and finally, temperature or molten jet effects. Chou et al. noted that any or all of these mechanisms could influence jet breakup. In later publications, Chou and Carleone (1977b) developed a one-dimensional Lagrangian theory for stretching plastic jets with a constitutive equation of the form

$$\sigma = \sigma_0 + C\varepsilon + R\varepsilon^2 + \ldots\ldots,$$

where C, R, etc., are positive, empirical coefficients. The stretching jet problem assumed small surface disturbances and small strains. A stability analysis was performed using a linearized form of the one-dimensional model and a stability criterion was established. The theory showed that the disturbance growth rate in the jet increases as the wavelength of the disturbance decreases and as the stretching rate decreases. Also, for a perfectly plastic jet material, where $\sigma = \sigma_0$, the disturbance growth rate increases with increasing σ/ρ. All trends predicted by the one-dimensional theory were in agreement with two-dimensional hydrocode calculations. Also, the hydrocode calculations revealed the existence of a critical wavelength (i.e., disturbances having this wavelength will grow faster than all others) and showed that

elasticity effects and compressibility effects were nearly negligible. Additional details and analyses are given in Chou, Carleone and Karpp (1974) and Chou and Carleone (1976). Chou and Carleone (1977a, 1977b) provide details regarding the jet growth function and other factors affecting stability. Chou and his coauthors approached the calculation of the breakup time directly utilizing many flash radiographs of jets from shaped charge liners. The final results of the Chou-Carleone model for a copper jet reveal

$$\bar{t}_b = 3.75 - 0.125\ \bar{\dot{\varepsilon}}_o + \frac{1}{\bar{\dot{\varepsilon}}_o},$$

where $\bar{t}_b$ = dimensionless breakup time = $c_p\ t_b/r_o$; $c_p = \sqrt{\sigma/\rho}$; $\bar{\dot{\varepsilon}}_o$ = dimensionless strain rate = $\dot{\varepsilon}_o r_o/c_p$; and $\dot{\varepsilon}_o$ = initial strain rate = $\Delta V/\Delta X$; and t_b is the breakup time, σ is the yield strength, ΔV is the change in velocity, and ΔX is the change in length. The subscript o designates initial values when the liner element first arrives at the axis of symmetry. The numerical coefficients result from a curve fit of the dynamic ductility factor to experimental data. The details of this model and comparison with experimental data are summarized in Walters and Zukas (1989).

Recently, Chou et al. (1992) expressed the jet breakup time as

$$t_b = k\left(\frac{r_o^2}{c_p^2\,\dot{\varepsilon}_o}\right)^{1/3} = k\left(\frac{r_o^2\,t_o}{c_p^2}\right)^{1/3} = k\left(\frac{r^2 t}{c_p^2}\right)^{1/3},$$

where the radius r and time t of a jet segment may be taken at any time before jet breakup. The factor k is taken to be 5.0 based on a fit of the equation with experimental data. The term c_p is defined as before, but σ is the yield stress (σ_y) for an isotropic jet and σ_y (0.5 + $1/m^2$) for an anisotropic jet, where m is the ratio of transverse strength to axial strength. Also, Rottenkoller (1989) obtained a similar formula for the breakup time of a shaped charge jet,

$$t_b - t_o = \left(\frac{d_o^2}{\dot{\varepsilon}_o\,c_p^2\,B^2}\right)^{1/3},$$

where d_o is the initial jet diameter, and B is equal to $\dot{\epsilon}d/c_p$ and assumed to be constant.

Eitan Hirsch (1979) expressed the breakup time as

$$\tau = \frac{\sqrt{8Rt}}{V_{pl}} \sin \frac{\beta}{2} = d_{jo}/V_{pl},$$

where d_{jo} is the initial jet diameter when elongation starts, R is the radius of the liner element, t is the thickness of the element, β is the collapse angle, τ is the breakup time measured from the arrival of the explosive wave front at the liner element from where the jet originates, and V_{pl} is a velocity specified by the liner material, called the "plastic velocity." Hirsch (1979) expressed the plastic velocity as the velocity difference between the jet particles or $V_{pl} = (V_j - V_r) / n$, where n is the number of jet particles, V_j is the jet tip velocity, and V_r is the velocity of the rear of the jet. Hirsch also gave expressions for the breakup time of an expanding cylinder (pipe) and a linear shaped charge. Hirsch (1989) attempted to express the plastic velocity as

$$V_{pl} = \sqrt{\sigma/\rho},$$

where σ is the liner metal dynamic yield stress and ρ is the density of the liner material, from microscopic metallurgical conditions. Hirsch employed the Mott fragmentation model as mentioned by Chou et al. (1963) and provided a description of the breakup time model as arising from shear bands or

$$V_{pl} = \sqrt{d\sigma_m/\rho},$$

where $d\sigma_m$ represents the difference between the isothermal and adiabatic stress vs. strain characteristics of the metal at the point where adiabatic stress becomes a maximum. Hirsch quotes strains of 1 to 2 at a strain rate of 10^5 s^{-1} for OFHC copper. These values of strain are considerably lower than those quoted by Chou and Carleone (1976). Hirsch (1981a) further qualified the plastic velocity by suggesting a breakup mechanism, where holes caused by a pile up of vacancies are formed at the metal surface and gradually increase until breaking is caused by the formation of voids in the jet. Hirsch also predicted the existence of a strain rate threshold below which other mechanisms dominate the breakup process. Hirsch

(1981b) states that even perfectly symmetrical and homogeneous shaped charge configurations have transverse velocity components in the jet. This means that the breakup process starts during the liner collapse and the transverse velocity influences the jet breakup. Hirsch (1990) relates the plastic velocity to the processes which affect the liner metallurgical state during the initial stages of jet formation. Hirsch shows how both the deformation energy heating the sliding shear bands during the localization process and the rate of the instability growing in the plastic flow during this process, combine to determine the plastic velocity parameter. This velocity is shown to be related to both the velocity due to the plastic deformation and the component of the maximum slide velocity allowable to form shear bands in the elongation direction. Hirsch thus attempts to include the influence of the metallurgical structure of the liner on the breakup time. In this study, small strains (less than 1) are calculated.

Haugstad (1983) and Haugstad and Dullum (1983) formulated two models for the jet breakup time by considering viscoplastic effects or $\sigma = \sigma_o + \mu\dot{\epsilon}$, where μ has the form of a viscosity, σ is the yield stress, σ_o is the quasistatic yield stress, and $\dot{\epsilon}$ is the strain rate. They obtained

$$t_b = \frac{\alpha d_o}{\sqrt{\sigma_o/\rho}} - \frac{1}{\dot{\epsilon}_o},$$

in the limit as $\mu \rightarrow 0$, where d_o is the initial jet diameter and α is a constant. Note that if

$$V_{pl} = \frac{\sqrt{\sigma/\rho}}{\alpha},$$

a modified Hirsch model results. The second (viscoplastic) model gave

$$t_b = b\,\mu/\sigma_o - 1/\dot{\epsilon}_o,$$

where b is a constant.

Pfeffer (1980) obtained a jet breakup time formula which indicates the breakup time is inversely proportional to the initial strain rate, weakly dependent on the initial jet radius, but independent of the liner material yield strength. Pfeffer gives

$$t_b = 1.4/\dot{\epsilon}_o + 48.5\ r_o/C_o,$$

where $\dot{\epsilon}_o$ is the initial strain rate, r_o is the initial jet radius, and C_c is the shock velocity in the jet. Pfeffer assumed a formula for the shape of the broken jet segment and his results are based on a curve fit of two-dimensional computer simulations.

Held (1989) and Mayseless et al. (1989) (as well as the Soviet researchers) advocate a calculation of the breakup distance instead of the breakup time. Walters and Summers (1992a) derived the formula of Mayseless et al. (1989) from the velocity difference expressions shown in Walters and Summers (1992b) and assuming simple tension. Held, Mostert and Koenig, Golaski and Duffy, and Hirsch, among others, comment on the influence of liner metallurgy on the jet breakup time. Golaski and Duffy (1987) did not provide a breakup time formula, but showed a direct correlation between liner grain size and jet breakup time. Mostert and Koenig (1987) claimed that the jet from a shaped charge elongates to a strain well in excess of 10 before it particulates. They also noted that the micromechanical properties of the liner, as well as its purity, have an influence on the ductility of the jet, but these factors are not included in the existing breakup models. Mostert and Koenig expressed the breakup time, τ, as

$$(\tau + \ell_o/V_o)^{3/2} - (\ell_o/V_o)^{3/2} = \left(\frac{3d_o}{8\alpha}\right)\sqrt{\ell_o/V_o}\ \ln(N_o/N_c),$$

where the jet has an initial diameter d_o and an initial length ℓ_o. V_o represents the velocity difference across the initial length and α is a proportionality constant. N_o is the initial moving-dislocation density immediately after jet formation and is influenced directly by the initial detonation shock pressure on the liner, the pressure experienced in moving through the collapse zone, and the effective pulse duration. Also, N_o varies inversely with the liner grain size. N_c is the postulated critical value of the moving-dislocation density where further elongation is inhibited. The value for the minimum density for plastic elongation could conceivably be linked to the value of the dynamic equilibrium density just prior to breakup.

However, all of these models are either incomplete or involve unknown material properties which are usually assumed to be constant, such as flow stress, dynamic viscosity or the like. Also, some models

involve unknown fitting parameters or variables. In addition, models, or observations, that seem acceptable for one liner geometry and material fail when applied to other geometries and/or liner materials. Thus, the various analytical models do not agree with each other or with the experimental data, and, in fact, the method of calculating jet breakup time distribution from the experimentally obtained flash radiographs varies from institution to institution. Nevertheless, significant insight has been gleaned from the analytical breakup time models, namely, the existence of a critical wave length, the effect of jet strength (σ) and density (ρ), and the dependence on strain rate.

It is known experimentally that the jet microstructure, notably the grain size (and probably the grain size distribution, the grain orientation, the metal chemistry or purity, and the material texture) strongly affects the jet breakup time. In fact, Chokshi and Meyers (1990) point out that high strain rate deformation leads to an increase in temperature which, in conjunction with the large strains involved, leads to a very fine grain size microstructure due to dynamic recrystallization. Subsequently, the fine grain size leads to superplasticity at high strain rates, which in turn leads to large tensile strains to failure. However, these factors are not included in the analytical or theoretical breakup time models and including them is not straightforward. In fact, the underlying mechanisms behind jet breakup are not understood. If a known perturbation is applied to a stretching jet in a numerical experiment, the jet will neck at a critical wavelength and break. The exact nature and origin of this critical perturbation(s) is unknown, but may be due to irregularities in the liner material yield strength or other material or micromechanical properties, nonuniformities in the initial jet velocity gradient, jet surface roughness, or due to inherent perturbations in the fabrication of the shaped charge (e.g., material anisotropies, liner wall thickness variations, the quality of the liner inner surface and exterior surface, inhomogeneities in the explosive fill, etc.). Also, the exact nature of the fracture process (at a critical value of strain, pressure, stress, plastic work, or internal energy) is unknown. Furthermore, models that account explicitly for the nucleation and growth of voids, cracks, and shear bands have not yet matured to the extent that they can be readily incorporated into the hydrocode models.

Factors which are known to affect jet breakup time are given by Held (1989) and Walters and Zukas (1989). In general, the jet breakup time can be increased by decreasing the jet stretching rate, increasing the jet radius, increasing the jet density, decreasing the jet strength, and increasing the ductility of the jet under the dynamic conditions described above. Thus, the liner design, liner geometry, liner material, and method of fabrication of the shaped charge liner are all pertinent factors to be considered in assessing the jet breakup time distribution.

4. THE ANALYTICAL MODEL

In this section, an analytical model is developed for the breakup time of the jet from a shaped charge liner. The model is based on three presumptions. First, a kinematic expression for the breakup time; second an expression related to plastic stability; and finally, a material-based constitutive equation relating the stress, strain, strain rate, and temperature. In other words, the jet from a shaped charge liner will particulate when it becomes plastically unstable (Chou and Carleone 1977b), and the breakup time will depend on the stress, strain, strain rate, and temperature at failure (particulation).

Figure 5 illustrates the kinematic expression for the jet breakup time. An initial length of jet, ℓ_o, eventually stretches to length ℓ where it begins to neck at the breakup time, τ. Then

$$\ell = \ell_o + \tau(V_{jo} - V_R), \tag{1}$$

where V_{jo} is the tip velocity of the jet and V_R is the rear or tail velocity of the jet. Dividing Equation 1 by ℓ_o yields

$$\frac{\ell - \ell_o}{\ell_o} = \varepsilon_o = \frac{\tau(V_{jo} - V_R)}{\ell_o} = \tau \dot{\varepsilon}_o$$

or,

$$\tau = \frac{\varepsilon_o}{\dot{\varepsilon}_o}. \tag{2}$$

The plastic stability criterion requires that

$$\frac{d\sigma}{d\varepsilon} \geq \sigma \tag{3}$$

for stability, otherwise the jet necks and eventually breaks (Walters and Summers 1992a, 1992b). In order to implement the model, Equation 3 is used with the equality sign, or

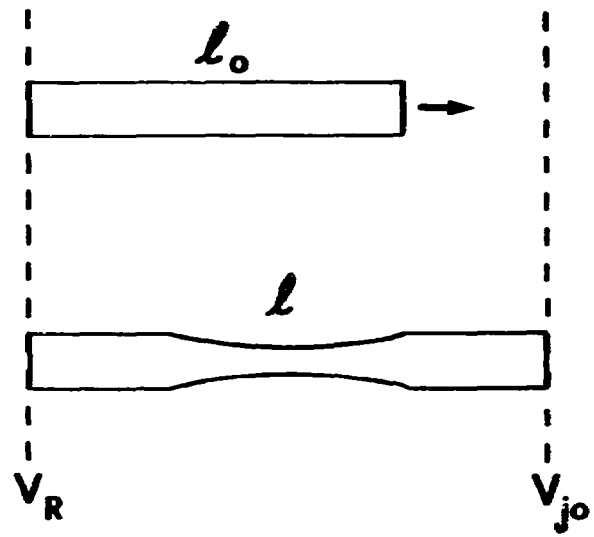

$$\ell = \ell_o + \tau (V_{jo} - V_R)$$

$$\frac{\ell - \ell_o}{\ell_o} = \varepsilon_e = \frac{\tau (V_{jo} - V_R)}{\ell_o} = \tau \dot{\varepsilon}_e$$

$$\tau = \frac{\varepsilon_e}{\dot{\varepsilon}_e}$$

Figure 5. The kinematic expression for the jet breakup time.

$$\frac{d\sigma}{\sigma} = d\varepsilon. \tag{4}$$

This is the same equation used to calculate the maximum load point. Equation 4 is integrated between the limits $\varepsilon = 0$ to $\varepsilon = \varepsilon_F$ and $\sigma = \sigma_o$ to $\sigma = \sigma_F$, where σ_o is the value of σ at $\varepsilon = 0$ and the subscript F denotes values at failure. Thus,

$$\frac{\sigma_F}{\sigma_o} = \exp \varepsilon_F. \tag{5}$$

Finally, a constitutive equation which relates stress, strain, strain rate, and temperature and is valid for high strain, strain rate, and temperature values is necessary. Such an equation may not exist for the extreme strains, strain rates, and temperatures the jet from a shaped charge liner is subjected to. Nonetheless, two constitutive equations were considered, Johnson-Cook (Johnson 1983; Johnson and Cook 1983, 1985) and Zerilli-Armstrong (1987), due to their popularity in many hydrocodes and the fact that the material coefficients are available for most materials of interest in shaped charge liner design.

The Zerilli-Armstrong (1987) constitutive equation for face-centered-cubic materials is

$$\sigma = C_o + k\lambda^{-1/2} + C_2\varepsilon^{1/2}\exp(-C_3T + C_4T\ln\dot{\varepsilon}). \tag{6}$$

The stress σ is in MPa, the strain rate $\dot{\varepsilon}$ is in s^{-1}, and the temperature T is in K. For an OFHC copper jet, Zerilli-Armstrong gives:

k = microstructural stress intensity = 5.0 MPa $(mm)^{1/2}$
λ = grain size = 0.075 mm
C_o = 46.5 MPa
C_2 = 890.0 MPa
C_3 = 0.0028 K^{-1}
C_4 = 0.000115 K^{-1}.

The Johnson-Cook (1983, 1985) constitutive equation, which has a different functional form as compared to the Zerilli-Armstrong equation is

$$\sigma = (A + B\varepsilon^n)(1 + C \ln \dot{\varepsilon})(1 - T^{*m}), \tag{7}$$

and

$$T^* = (T - T_{room})/(T_{melt} - T_{room}),$$

$$0 \leq T^* \leq 1,$$

where for OFHC copper,

$$T_{melt} = 1{,}356 \text{ K}, \; T_{room} = 293 \text{ K}, \; C = 0.025,$$

$$m = 1.09, \; n = 0.31, \; A = 90.0 \text{ MPa, and } B = 292.0 \text{ MPa}.$$

Note that in the system of units used in the above equations, the density, ρ, of copper is 8,960 kg/m^3. In addition, the modified Johnson-Cook model was examined. The modified Johnson-Cook equation is

$$\sigma = (A + B\varepsilon^n)\dot{\varepsilon}^c(1 - T^{*m}), \tag{8}$$

where, for OFHC copper, all constants have the same value as in the original Johnson-Cook model, but the functional form of the strain rate dependency has been changed. Any constitutive equation may be used in this analysis, assuming of course that the parameters used in the equation are available and do not introduce additional unknowns (such as the pressure for example).

The true strain at failure, ε_F, is determined using Equation 5 and a constitutive equation (e.g., Equations 6–8). The value of σ_0 is calculated as:

$$\sigma_0 = C_0 + k\lambda^{-1/2}$$

from Equation 6 for the Zerilli-Armstrong constitutive equation for face-centered-cubic materials. For the Johnson-Cook constitutive model, Equation 7,

$$\sigma_0 = A(1 + C \ln \dot{\varepsilon})(1 - T^{*m}).$$

In addition, the true strain rate, required in the constitutive equations, is determined as a function of the true strain using

$$\dot{\varepsilon} = \dot{\varepsilon}_0 \exp(-\varepsilon)$$

as derived in Walters and Summers (1992b) under the assumption of a constant jet stretching rate. Finally, the jet temperature is assumed to be established at failure and is constant. Thus, the final true strain at failure and the true stress at failure may be determined given an initial strain rate and an assumed jet temperature.

The initial strain rate is given as

$$\dot{\varepsilon}_0 = \frac{\Delta U}{\ell_0},$$

where

$$\Delta U = V_{j0} - V_R$$

and

V_{j0} = the jet tip velocity,
V_R = the velocity of the rear of the jet.

The velocity difference, ΔU, can be calculated using the methods given in Walters and Zukas (1989), for example, and is considered known. The initial jet length, ℓ_o, is taken to be the initial length of the jet available prior to stretching. For a conical liner, ℓ_o is determined based on the slant length of the cone. This is essentially the jet length considered in the steady state jet formation theory of Birkhoff, MacDougall, Pugh, and Taylor described in Walters and Zukas (1989). For nonconical liners, ℓ_o is based on one-half the perimeter of the inside surface of the liner obtained by taking a cross section along the axis of the liner. In general, the initial jet length is taken as:

$$\ell_o = \ell_s \left(\frac{V_{jo} - V_R}{V_{jo}} \right),$$

where ℓ_s is the slant height or one-half the liner perimeter and V_R is the measured tail velocity from the flash x-ray of the jet (which depends on the length of jet captured on the film). Thus,

$$\dot{\varepsilon}_o = \frac{V_{jo}}{\ell_s}.$$

The ratio $(V_{jo} - V_{rear})/V_{jo}$ is introduced to account for the fact that the flash radiograph may not provide information on the entire length of the shaped charge jet. However, this ratio does not account for the portion of the apex region of a conical liner which only contributes to the mass of the jet tip particle or the portion of the base region of the liner which does not contribute to the jet.

The Johnson-Cook constitutive equation yielded very low values for the strain at failure (as compared to the Zerilli-Armstrong constitutive equation). Also, because of the functional form of the Johnson-Cook equation, the strain at failure is independent of the temperature and strain rate. The same statements apply to the modified Johnson-Cook constitutive equation (Equation 8). Thus, the Johnson-Cook based results will not be presented. The low strains obtained by the Johnson-Cook model were also observed by and reported in Walters and Summers (1992b).

Figure 6 plots the final true strain, ε_F, as a function of the initial strain rate, $\dot{\varepsilon}_o$, with temperature as a parameter. The experimental data points are plotted for several different conical liner designs as well

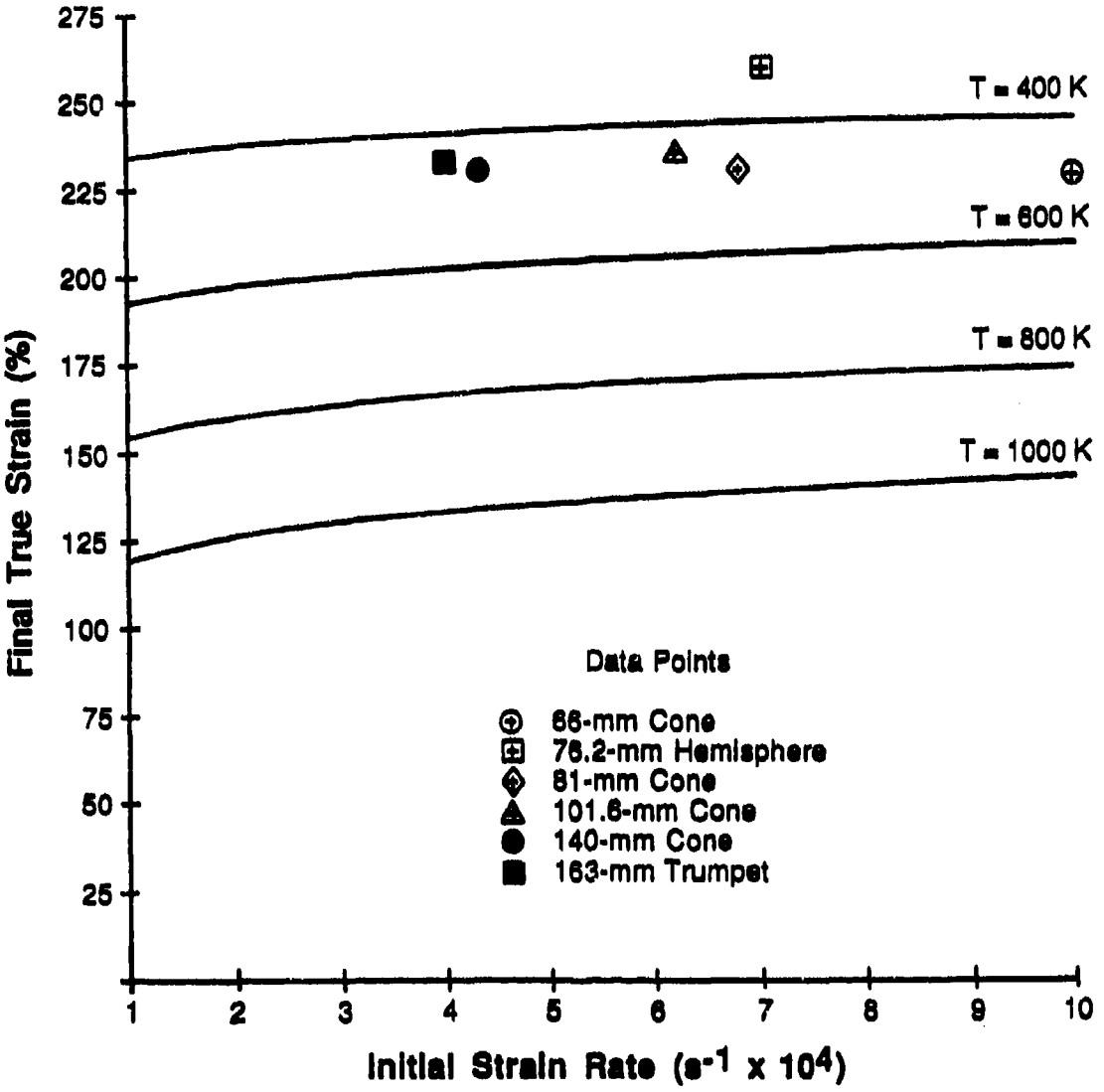

Figure 6. The final true strain vs. the initial strain rate with temperature as a parameter for several copper shaped charge liner designs.

as a trumpet and a hemispherical liner configuration. In all cases, the liner material was copper. The experimental points were determined based on the calculated initial length, ℓ_0, and the total jet length, L, measured directly from the flash radiographs of the jet. Note that for the conical and trumpet liners the average final true strain of the jet is nearly constant or

$$\varepsilon_F = \ln \frac{L}{\ell_0} \approx 2.3 .$$

For an average final true strain of 2.3,

$$\exp \varepsilon = \frac{A_0}{A} = \left(\frac{r_0}{r}\right)^2$$

for cylindrical jet particles, or $r/r_0 = 0.32$.

For the hemispherical liner, the average final strain is higher, about 2.5. This difference in final true strain values may well be due to the different jet collapse and formation mechanisms between hemispherical and conical (or conical-like) liners or it may relate to the method used to calculate ℓ_0 (as one-half of the perimeter of the inside surface of the liner) for hemispherical liners. Note that this plot would seem to indicate that the jet temperature would be around 450 K to 500 K for the conical liners and somewhat lower for hemispherical liners based on the constitutive equation used for copper. Note also that for any given temperature, the final true strain is nearly constant with strain rate.

Table 1 presents the experimentally determined jet tip velocity, jet tail velocity, total jet length, and cumulative jet breakup time for several conical liner designs, a trumpet liner design, and a hemispherical liner design. The calculated total length and cumulative breakup time are also shown for comparison. The results presented in Table 1 show excellent agreement with the experimental data at a temperature of 450 K. The experimental breakup time is derived from the virtual origin approximation, which gives $\ell = \ell_0$ at the virtual origin time t_0. Thus, assuming $t_0 = 0$,

$$\tau_e = \frac{L}{(V_{jo} - V_r)} = \frac{1}{\dot{\epsilon}}.$$

Then, if $\epsilon_o \neq 0$, it follows that

$$\tau_e = \frac{\epsilon_e + 1}{\dot{\epsilon}_o}. \tag{9}$$

The calculated values given in Table 1 were computed using Equation 9.

Table 1. A Comparison Between the Experimental and Analytical Values of Total Jet Length and Cumulative Jet Breakup Time for Several Shaped Charge Liner Designs

	65.3-mm Cone	76.2-mm Hemi	81-mm Cone	101.6-mm Cone	140-mm Cone	163-mm Trumpet
V_{TIP} (km/s)	9.2	4.2	7.7	8.8	8.5	10.0
V_{TAIL} (km/s)	4.2	2.4	2.1	4.3	2.6	4.7
L_T (mm)	500.1	279.9	820.3	772.1	1,350.7	1,363.2
T_B (μs)	99.2	160.9	147.8	169.3	231.3	255.8
Predictions T = 450 K						
L_T (mm)	530.4	260.1	849.3	758.5	1,366.5	1,341.7
T_B (μs)	105.2	149.5	153.0	166.3	234.0	251.7

Next, the cumulative jet breakup time is plotted as a function of charge diameter for various temperatures in Figure 7. This plot was constructed by holding the jet tip and tail velocities constant and varying the liner diameter. In this case, the experimental results from the 81-mm conical liner were used. The measured average breakup time was 147.8 μs for this round, as plotted on Figure 7. The dashed line represents the breakup time which would be attained if homologous scaling is assumed. In fact, homologous scaling of the jet breakup time has been experimentally observed to be a good assumption, usually accurate to within ±20%. Figure 7 shows that scaling appears to exist at temperature of 400 K to 500 K more so than at higher temperatures (i.e., the slope of the scaling [dashed] line matches the slope of the 400-K line).

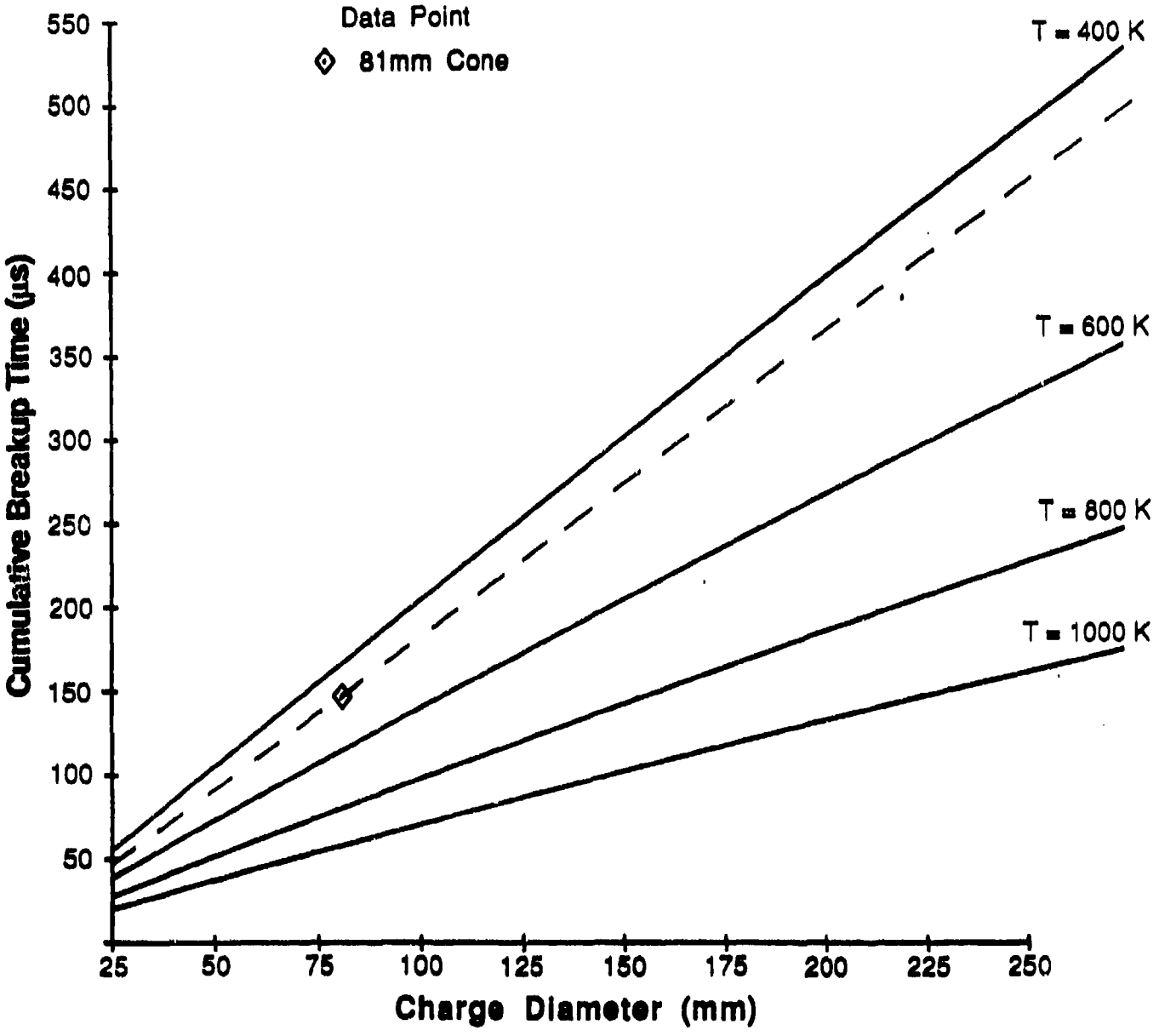

Figure 7. Cumulative jet breakup time vs. charge diameter with temperature as a parameter.

Figure 8 shows the predicted variation of the cumulative jet breakup time with temperature for a 81-mm diameter shaped charge with a copper conical liner. Note the ductility of the jet is expected to decrease with increasing jet temperature. This is due to the constitutive equation and the observation that, for face-centered-cubic materials, the strain at maximum load decreases with increasing temperature (Zerilli and Armstrong 1987).

The calculation of ℓ_0 and $\dot{\varepsilon}_0$, based on the slant height of the liner and the tip to tail velocity difference, allows a quick calculation of the total jet length and cumulative breakup time. However, this method only provides a prediction of the average strain attained by the entire jet and a single cumulative breakup time. Alternately, this model may be employed in conjunction with a jet formation code. In the jet formation code, the value of ℓ_0 is defined to be the length of a segment of the jet at the time it reaches the liner axis of symmetry. The velocity difference, used to calculate initial strain rate, is defined as the velocity of the proceeding jet segment less the velocity of the succeeding element. The use of the breakup time model in conjunction with a jet formation model also allows for the prediction of individual breakup times, actual separation times, and the distance a segment of jet travels before particulation.

Figures 9–12 repeat the experimental data shown in Figures 1–4 for the 81-mm copper conical shaped charge liner. The analytical predictions, using the jet formation code, are also shown on these plots for a temperature of 450 K. Figure 9 is a plot of the cumulative breakup time vs. the jet tail velocity. As shown in Figure 9, the amount of the jet which is characterized can significantly influence the measured value of breakup time. The extremely high breakup time values predicted in the tip region of the jet are due to the mass buildup, or inverse velocity gradient, which forms the tip particle. Large initial values of jet breakup are measured experimentally, although the deceleration of the tip may be a factor. Extremely high values of breakup time are also predicted for very low jet tail velocities but these are probably an artifact of the jet formation code since some portion of the liner (near the base) may not actually contribute to the jet.

Figure 10 shows the individual breakup time, calculated between the centers of mass of adjacent jet particles, vs. the jet velocity. The experimental data points show a large amount of scatter. The scatter is primarily due to variations in the velocity difference between the adjacent particles, as was also shown in Walters and Summers (1992b).

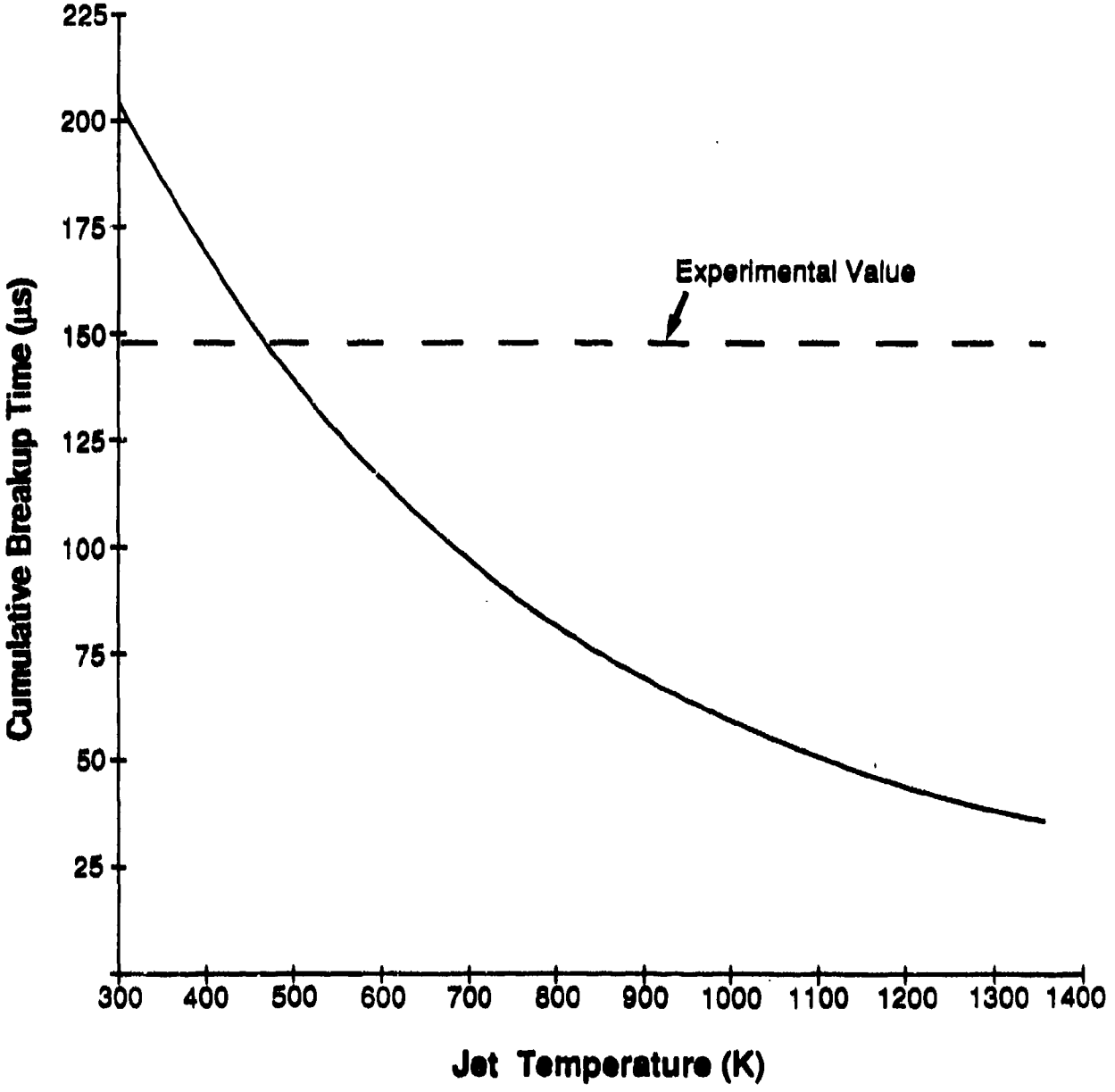

Figure 8. Cumulative breakup time as a function of jet temperature for the 81-mm shaped charge with a copper conical liner.

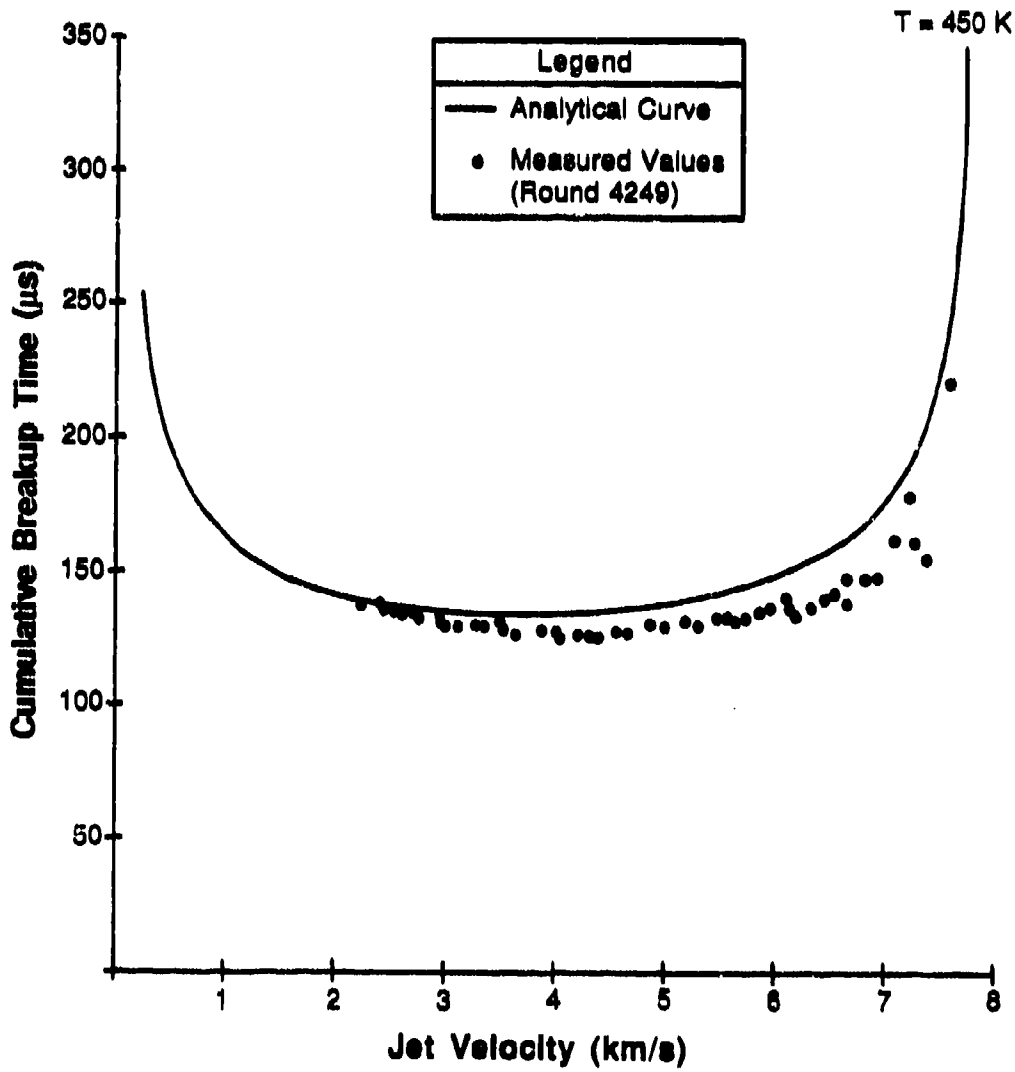

Figure 9. Cumulative breakup time as a function of jet velocity for the 81-mm shaped charge.

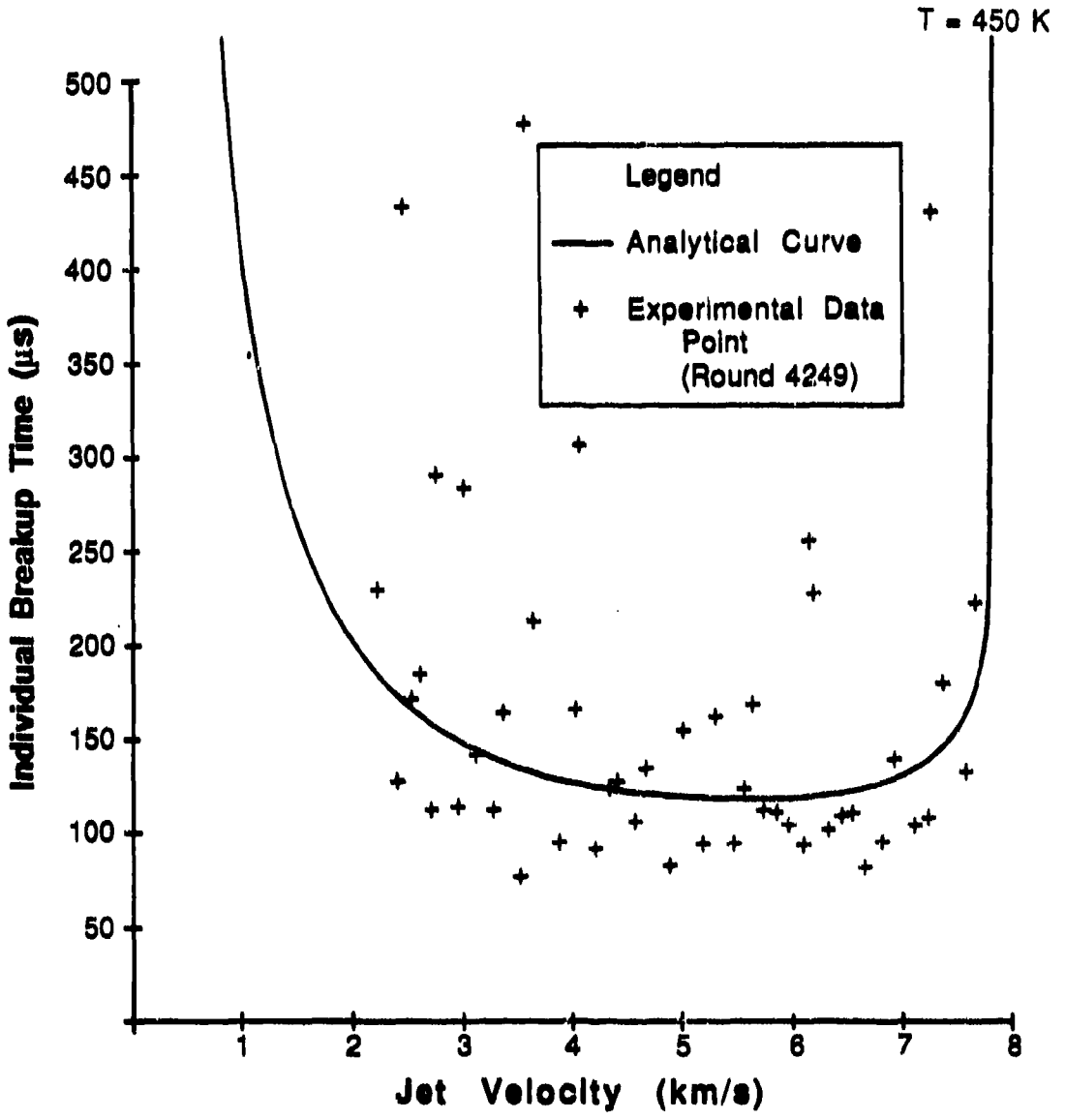

Figure 10. Individual breakup times as a function of jet velocity for the 81-mm shaped charge.

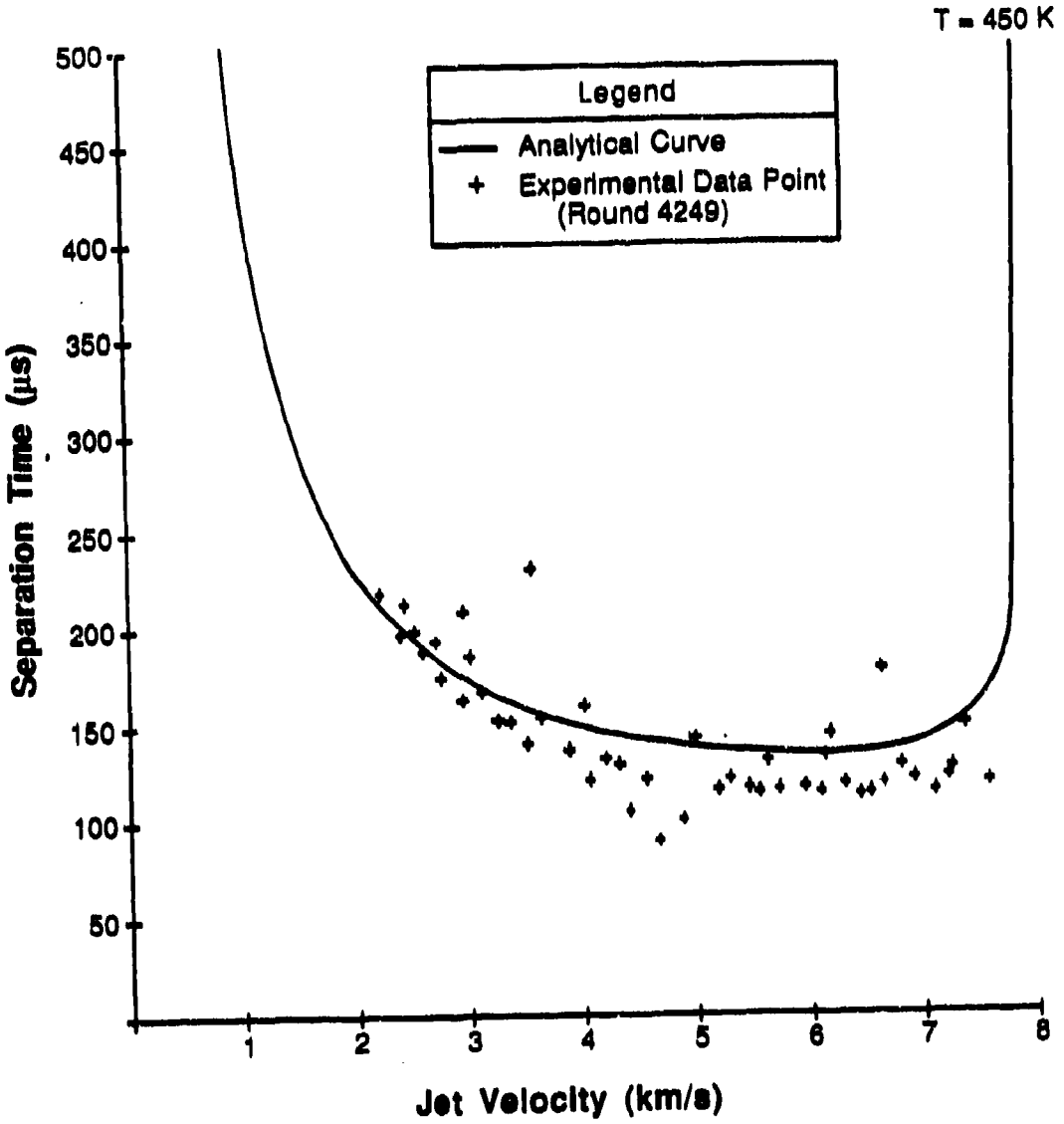

Figure 11. The separation time of each jet particle as a function of jet velocity for the 81-mm shaped charge.

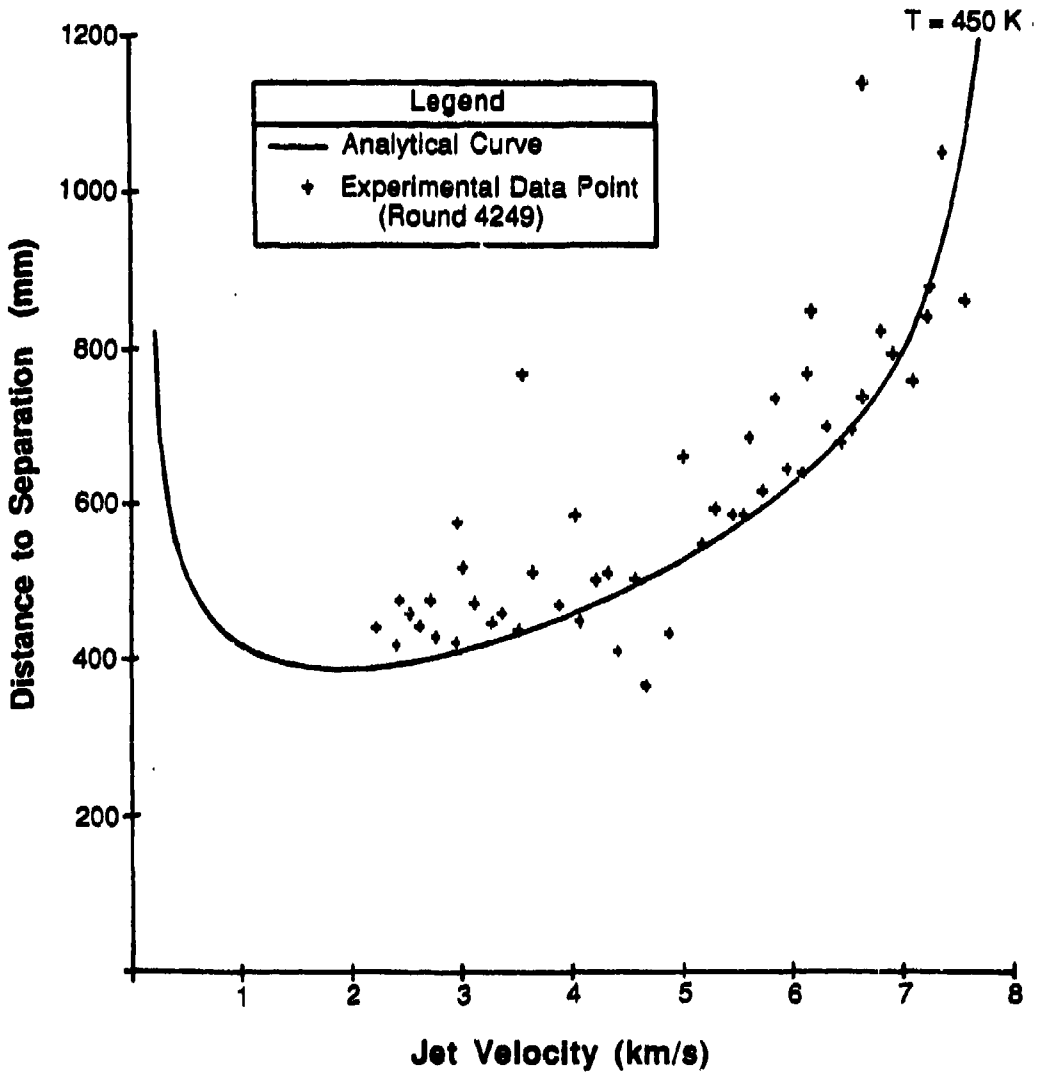

Figure 12. The distance travelled before particulation vs. jet velocity for the 81-mm shaped charge.

Figures 11 and 12 are plots of separation time vs. jet velocity and the distance a jet particle travels before separation vs. jet velocity, respectively. Figure 11 indicates the actual particulation time tends to increase with decreasing jet velocity. It is not evident that the jet breakup proceeds uniformly from the tip to tail. The model predicts a first break near the front of the jet but away from the tip region for the warhead designs considered in this study. The analytical prediction agrees well with the experimental data, however, the model is clearly not sophisticated enough to predict the variations which occur, from particle-to-particle, in individual breakup time, separation time, or separation distance. Also, simple jet formation codes are not valid for hemispherical liners, but hydrocode simulations could readily be employed to determine the length of various segments of the jet at the time they reach the axis of symmetry.

Figures 13–16 show a similar comparison between analytical and experimental data for the 140-mm conical liner. The agreement between calculated and experimental values is quite good at the jet tail for a jet temperature of 450 K. However, the analytical predictions are not as good near the front of the jet unless the jet temperature is increased to 650 K. This discrepancy may indicate a temperature gradient exists along the jet (from the tip to the tail) with the jet tip at a higher temperature. Table 2 lists the predicted tip velocity, total jet length, and cumulative breakup time for each of the conical liners shown in Table 1. The total jet length and cumulative breakup time predictions are given for the same approximate velocity gradient as those given in Table 1.

As shown earlier, the calculated breakup time results match the experimental data quite well at an assumed uniform temperature of 450 K. This temperature is below the measured values of von Holle and Trimble (Walters and Zukas 1989) for a shaped charge with a copper, conical liner. However, the experimental temperature measurements were taken near the tip region of the jet. There may be a temperature gradient along the length of the jet (from tip to tail) as well as a temperature gradient through the jet thickness. A temperature gradient from the jet tip to the jet tail could result in lower temperatures near the rear of the jet which perhaps undergoes less plastic deformation and less shock heating than the jet tip region. Ideally, the individual breakup time could be calculated from a jet formation code with temperatures for each element of the jet (obtained from hydrocode calculations perhaps) used as input.

The breakup model in conjunction with the jet formation model predicts the true strain at failure as approximately 2.3. This value is an average value calculated for discrete jet segments. Stress concentrations in the necked regions of the jet are not included in the model nor are release waves or liner

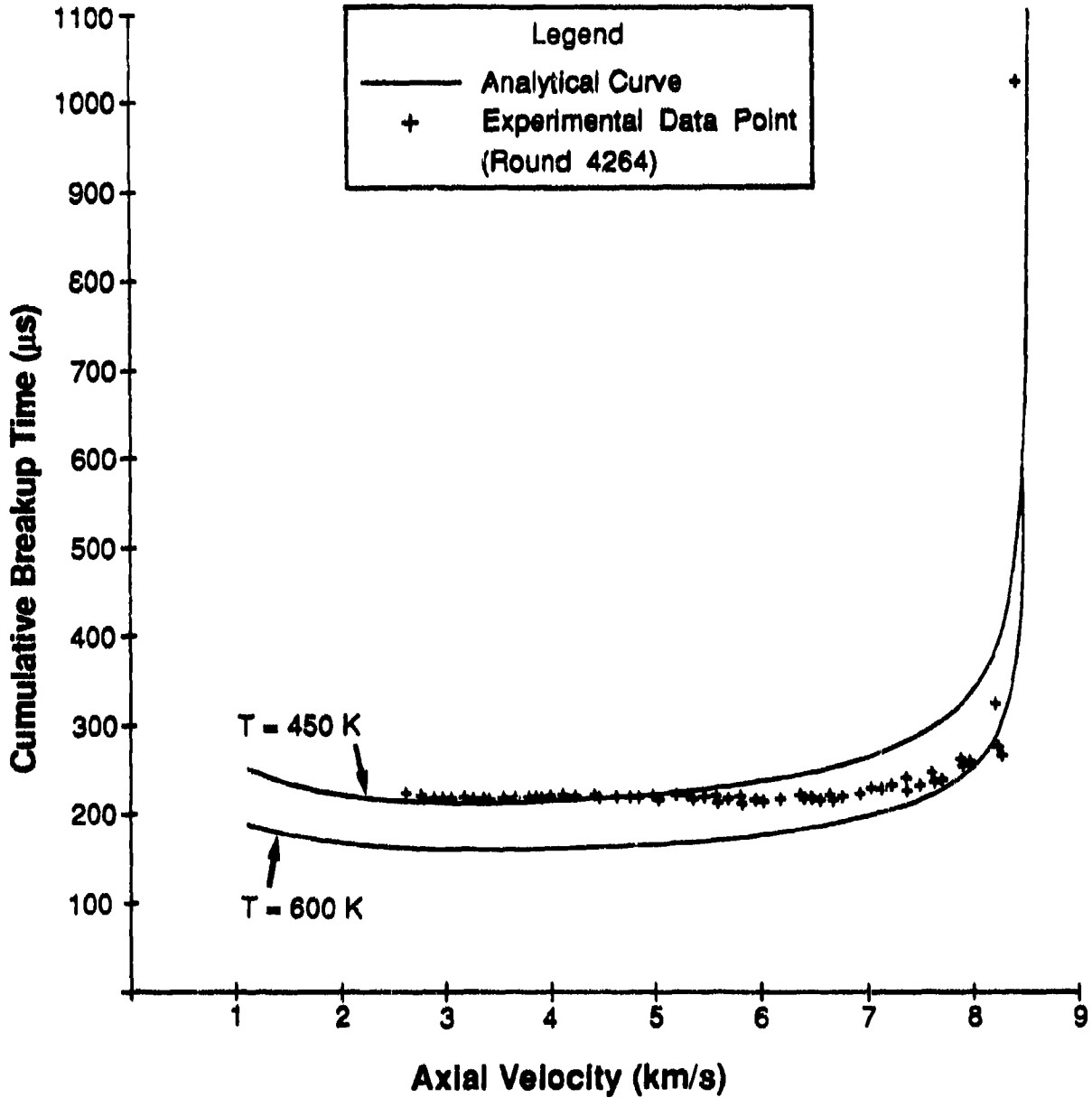

Figure 13. Cumulative breakup time as a function of jet velocity for the 140-mm shaped charge.

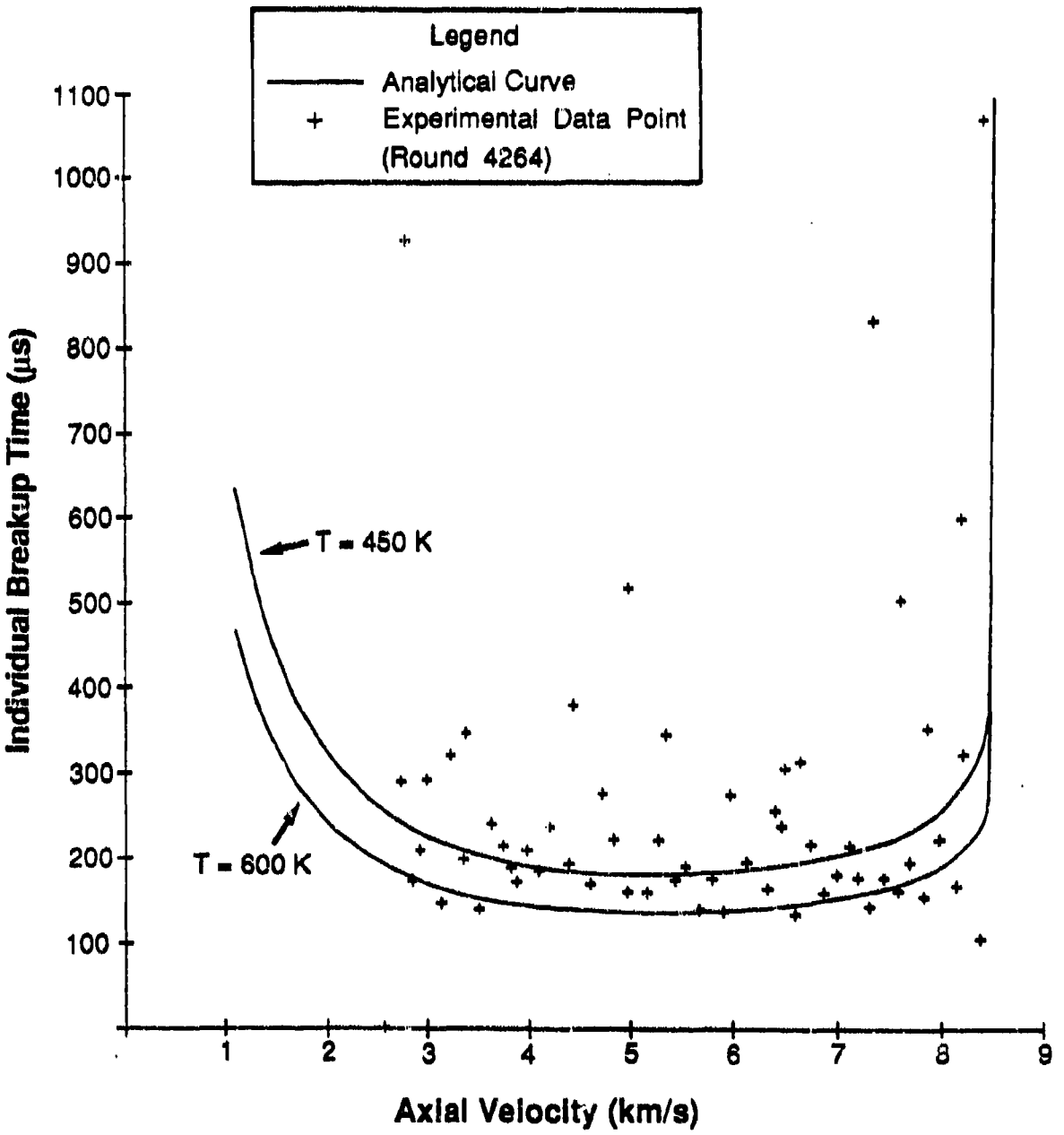

Figure 14. Individual breakup times as a function of jet velocity for the 140-mm shaped charge.

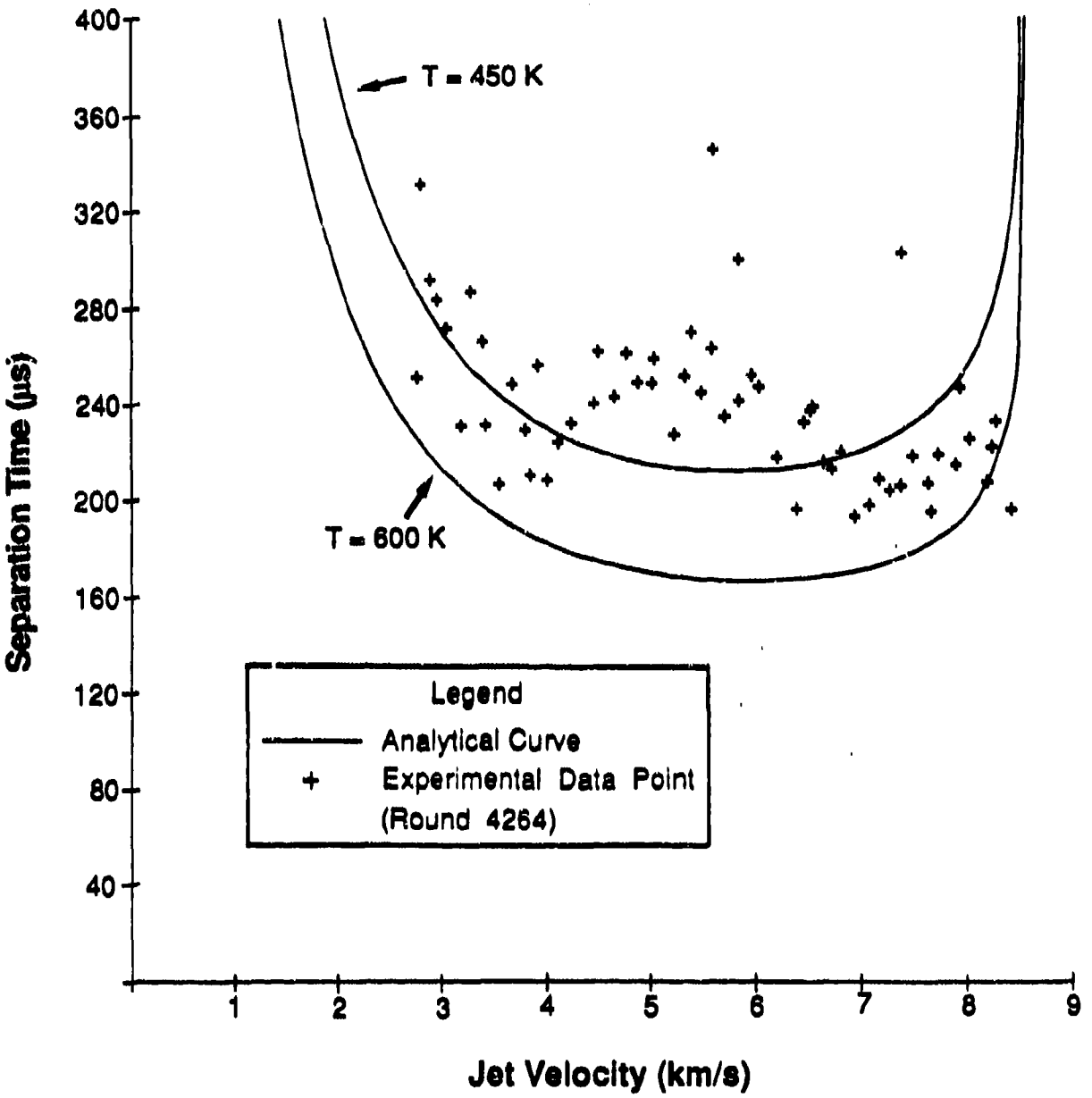

Figure 15. The separation time of each jet particle as a function of jet velocity for the 140-mm shaped charge.

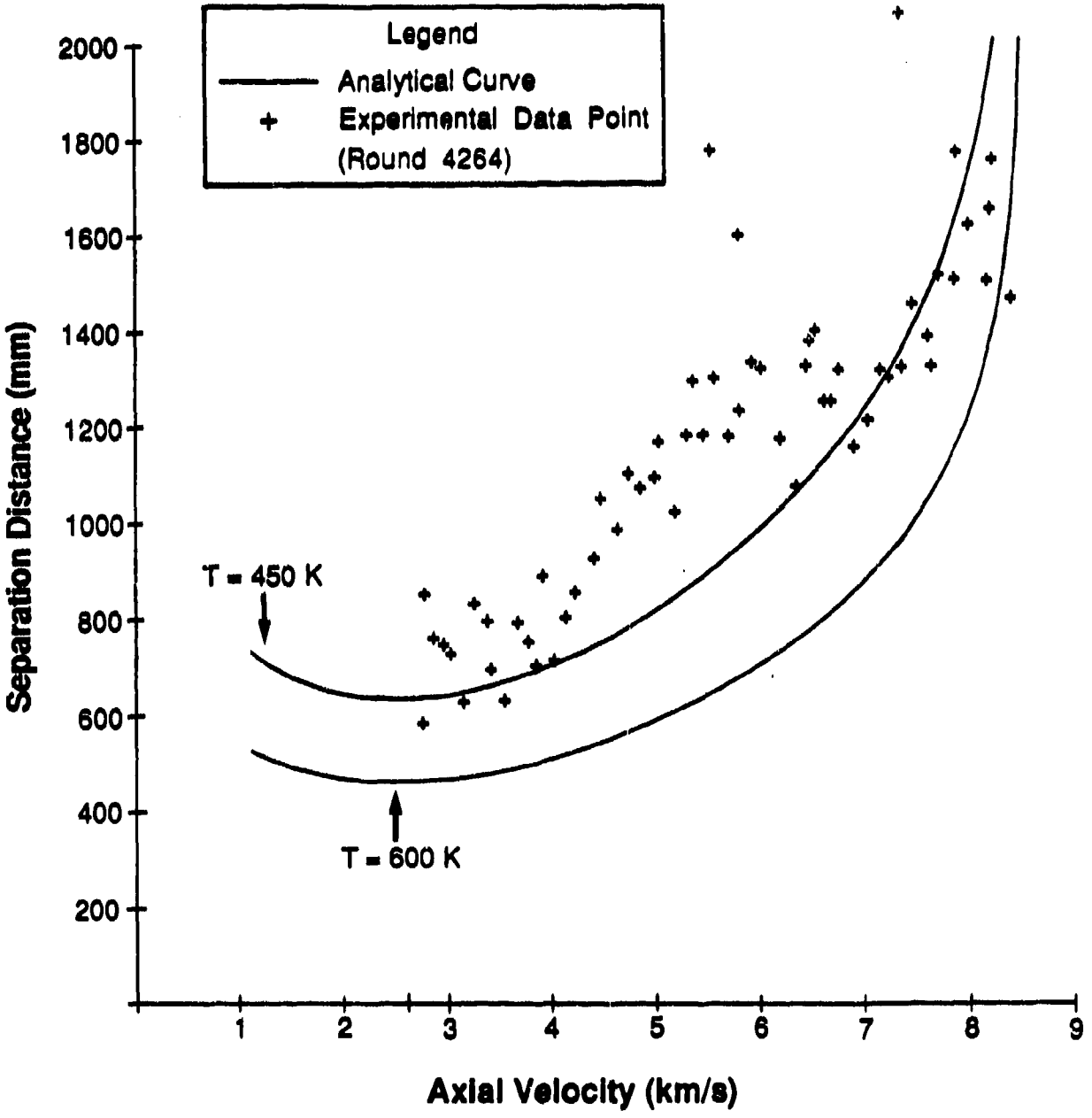

Figure 16. The distance travelled before particulation vs. jet velocity for the 140-mm shaped charge.

Table 2. Jet Formation Code Predictions for a Temperature of 450 K

	65.3-mm Cone	81-mm Cone	101.6-mm Cone	140-mm Cone
V_{TIP} (km/s)	9.2	7.8	8.9	8.5
V_{TAIL}* (km/s)	4.3	2.1	4.2	2.6
L_T (mm)	508.2	808.4	730.3	1,267.1
T_B (μs)	101.9	140.4	154.6	215.0

* The tail velocity was chosen to approximate the velocity of the last particle characterized in the experiments of Table 1.

inhomogenities. Other fracture models (e.g., Johnson [1983]) may provide a more accurate strain at the actual break point between jet particles. However, such a calculation would require a hydrocode solution.

It is also worthy of mention that the Zerilli-Armstrong constitutive equation has been extended beyond its intended range of applicability for the high temperatures and strain rates the jet material undergoes during the formation and particulation process. Also, it has been postulated that an increase in strain rate is equivalent to a decrease in temperature (Johnson and Mellor 1973). Thus, in the constitutive equation used in this study, the high strain rate effects may overshadow the temperature influence.

5. DISCUSSION

As stated earlier, the average true strain of the shaped charges with conical or conical-like liners is approximately 2.3. An alternative failure model may simply be to set the strain at failure to 2.3. In this case, *a priori* knowledge of the jet temperature is not required. Figure 17 is a plot of the value of true stress predicted for a true strain of 2.3 as a function of jet temperature for both the Zerilli-Armstrong and Johnson-Cook constitutive equations. Other researchers have claimed failure occurs at a stress of 300 MPa for a copper jet (Walters and Summers 1992a). The Zerilli-Armstrong constitutive equation predicts a stress of 300 MPa when the jet temperature is approximately 980 K. The Johnson-Cook model predicts a stress of 300 MPa for a jet temperature of approximately 830 K. Both of these jet temperatures seem high compared to the measurements of von Holle and Trimble.

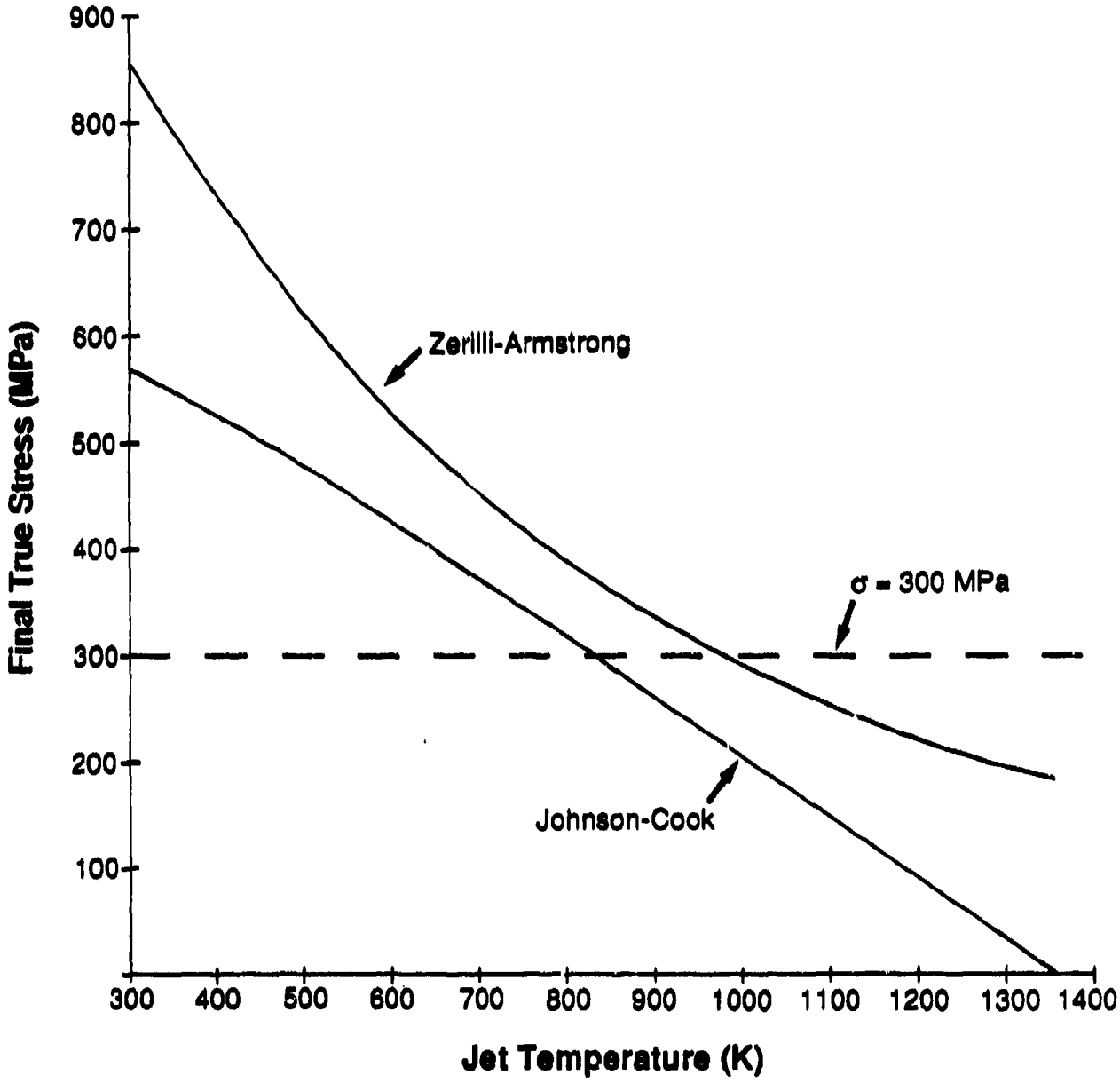

Figure 17. Final true stress vs. jet temperature for the 81-mm conical liner and a final true strain of 2.3.

Alternatively, the stress at failure may be set to 300 MPa. Figure 18 shows the values of strain at failure as a function of jet temperature given by the Zerilli-Armstrong and Johnson-Cook constitutive equations for the 81-mm shaped charge. Again, reasonable jet breakup times are achieved when the true strain is approximately 2.3. This failure criteria gives reasonable jet temperatures, but the strain at failure is extremely sensitive to jet temperature. A constant stress failure criterion reverses the trend shown in the previous section (i.e., the true strain at failure increases with increasing jet temperature). In addition, the trends predicted using the Johnson-Cook model are in agreement with those of the Zerilli-Armstrong constitutive equation for both the constant stress and constant strain failure criterions. For other liner materials, a procedure similar to that used in this study can be employed to obtain a new critical strain. This strain value is then constant for a given liner material and geometry.

6. CONCLUSIONS

A technique was derived to calculate the breakup time for a shaped charge with a face-centered-cubic liner material. The approach involved an equation for plastic instability; a kinematic relationship for the jet breakup time; and a material-dependent constitutive equation. The study was limited to data which the authors had personally analyzed since there are several possible ways to express a distribution of jet breakup times and it is often not clear as to the time origin involved or the experimental data reduction methods used. Also, the constitutive equation used must be expressed in terms of known coefficients. For example, molybdenum was not addressed in this study since the Zerilli-Armstrong coefficients are not yet available for this material.

The jet breakup time predictions were shown to be very good for several shaped charge designs with copper liners. Using the model in conjunction with a jet formation code revealed good agreement between calculated and experimental jet breakup time distributions for an assumed uniform temperature. The temperature is probably not uniform through the jet but the uniform value (450 K) used in this study seems to be low compared to the measurements of von Holle and Trimble.

The breakup time model was further simplified by noting that the average true strain at failure of all the copper shaped charge designs was approximately a constant, namely, 2.3. Also, a stress at failure may be selected (as 300 MPa) to yield another form of the simplified model.

Future studies will address body-centered-cubic shaped charge liner materials.

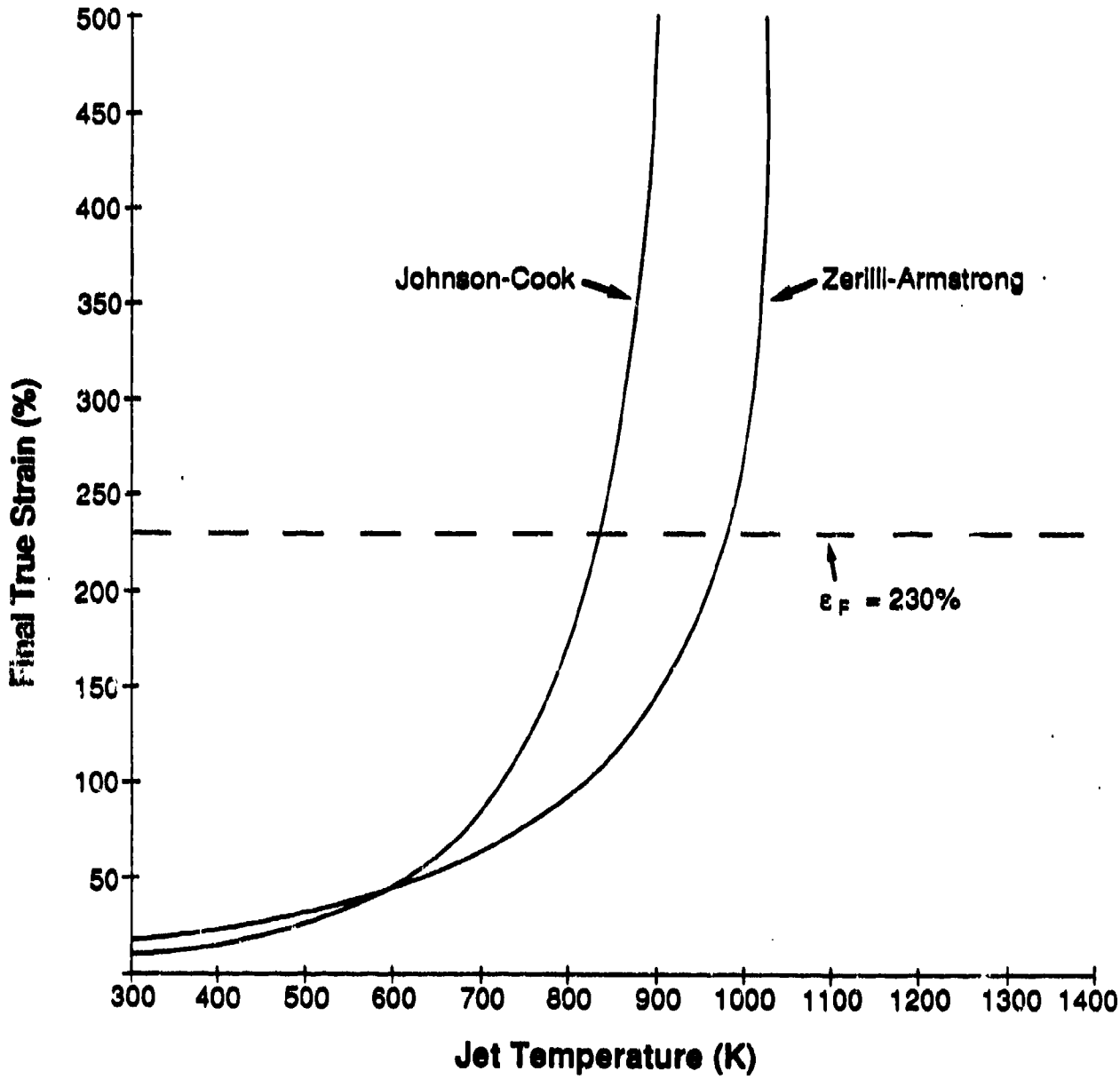

Figure 18. Final true strain vs. jet temperature for the 81-mm conical liner at a final true stress of 300 MPa.

7. REFERENCES

Chokshi, A. H., and J. A. Meyers. "The Prospects for Superplasticity at High Strain Rates: Preliminary Considerations and an Example." Scripta Metallurgica et Materialia, vol. 24, pp. 605–610, 1990.

Chou, P. C., and J. Carleone. "The Breakup of Shaped Charge Jets." Proceedings of the Second International Symposium on Ballistics, Daytona Beach, FL, March 1976.

Chou, P. C., and J. Carleone. "The Stability and Breakup of Shaped Charge Jets." Proceedings of the Third International Symposium on Ballistics, Karlsrue, Germany, March 1977(a).

Chou, P. C., and J. Carleone. "The Stability of Shaped Charge Jets." Journal of Applied Physics, vol. 48, no. 10, pp. 4187–4195, October 1977(b).

Chou, P. C., J. Carleone, and R. R. Karpp. "Study of Shaped Charge Jet Formation and Breakup." BRL-CR-138, U.S. Army Ballistic Research Laboratory, Aberdeen Proving Ground, MD, February 1974.

Chou, P. C., M. Grudza, Y. Liu, and Z. Ritman. "Shaped Charge Jet Breakup Formula with Metal Anisotropy," Proceedings of the 13th International Symposium on Ballistics, vol. 2, Stockholm, Sweden, 1–3 June, 1992.

Chou, P. C., H. S. Sidhu, and R. W. Mortimer. "A Study of the Breakup of Shaped Charge Jets." DIT Report No. 125-4, Drexel University, April 1963.

Curtis, J. P. "Axisymmetric Instability Model for Shaped Charge Jets." Journal of Applied Physics, vol. 61, no. 11, June 1987.

Frankel, I., and D. Weihs. "Stability of a Capillary Jet With Linearly Increasing Axial Velocity (With Application to Shaped Charges)." Journal of Fluid Mechanics, vol. 155, pp. 289–307, 1985.

Golaski, S. K., and M. L. Duffy. "Effect of Liner Grain Size on Shaped Charge Jet Performance and Characteristics." BRL-TR-2800, U.S. Army Ballistic Research Laboratory, Aberdeen Proving Ground, MD, April 1987.

Goldin, M., J. Yerushalmi, R. Pfeffer, and R. Shinnar. "Breakup of a Capillary Jet of a Viscoelastic Fluid." Journal of Fluid Mechanics, vol. 38, part 4, pp. 689–711, 1969.

Gordon, G. D. "Mechanism and Speed of Breakup of Drops." Journal of Applied Physics, vol. 30, no. 11, November 1959.

Gordon, P., R. Karpp, S. Sanday, and M. Schwartz. "Influence of Dynamic Yield Point in Multimaterial Impact." Journal of Applied Physics, vol. 48, no. 1, 1977.

Haugstad, B. "On the Break-up of Shaped Charge Jets." Propellants, Explosives, Pyrotechnics, vol. 8, pp. 119–120, 1983.

Haugstad, B., and O. Dullum. "The Jet Fragmentation Problem and Its Relation to Shaped Charge Engineering." Paper presented at MBB, Schrobenhausen, Germany, September 1983 (unpublished).

Heidmann, M. F., and J. F. Groeneweg. "Dynamic Response of Liquid Jet Breakup." AIAA Journal, vol. 6, no. 10, October 1968.

Held, M. "Determination of the Material Quality of Copper Shaped Charge Liners." Propellants, Explosives, Pyrotechnics, vol. 10, pp. 125–128, 1985.

Held, M. "Particulation of Shaped Charge Jets." Proceedings of the Eleventh International Symposium on Ballistics, Brussels, Belgium, May 1989.

Hirsch, E. "A Formula for the Shaped Charge Jet Break-up Time." Propellants, Explosives, Pyrotechnics, vol. 4, pp. 89–94, 1979.

Hirsch, E. "A Model Explaining the Rule for Calculating the Break-up Time of Homogeneous Ductile Metals." Propellants, Explosives, Pyrotechnics, vol. 6 pp. 11–14, 1981a.

Hirsch, E. "The Natural Spread and Tumbling of the Shaped Charge Jet Segments." Propellants, Explosives, Pyrotechnics, vol. 6, pp. 104–111, 1981b.

Hirsch, E. "The Mott Fragmentation Model and the V_{pl} Break-up Parameter." Propellants, Explosives, Pyrotechnics, vol. 14, pp. 31–38, 1989.

Hirsch, E. "The Effect of the Liner Metallurgical State on the Shaped Charge Jet Break-up Time." Propellants, Explosives, Pyrotechnics, vol. 15, pp. 166–176, 1990.

Hirsch, E. "Internal Shearing During Shaped Charge Jet Formation and Break-up." Propellants, Explosives, Pyrotechnics, vol. 17, pp. 27–33, 1992.

Johnson, G. R. "Development of Strength and Fracture Models for Computations Involving Severe Dynamic Loading Volume I: Strength and Fracture Models." AFATL-TR-83-05, Air Force Armament Laboratory, Eglin AFB, FL, January 1983.

Johnson, G. R., and W. H. Cook. Proceedings of the Seventh International Symposium on Ballistics. The Hague, The Netherlands, p. 541, 1983.

Johnson, G. R., and W. H. Cook. "Fracture Characteristics of Three Metals Subjected to Various Strains, Strain Rates, Temperatures, and Pressures." Engineering Fracture Mechanics, vol. 21, pp. 31–48, 1985.

Johnson, W., and P. B. Mellor. Engineering Plasticity, Ellis Horwood Limited, Chichester, 1973.

Mayseless, M., E. Marmor, S. Miller, B. Zommer. "A New Approach in Characterizing the Breakup Phenomenon of a Shaped Charge Jet." Proceedings of the Eleventh International Symposium on Ballistics, Brussels, Belgium, May 1989.

Mikami, T., R. Cox, and S. Mason. "Break-up of Extending Liquid Threads." Post-Graduate Research Laboratory Report, PGRL/72, Pulp and Paper Research Institute of Canada, October 1974.

Miller, C. "Generation of Necks in an Elongating Shaped Charge Jet." Proceedings of the Symposium on Ballistics, ADPA sponsored at the U.S. Army Ballistic Research Laboratory, Aberdeen Proving Ground, MD, November 1982.

Mostert, F. J., and P. J. Koenig. "A Link Between Liner Metallurgy and Shaped Charge Jet Ductility." South African Journal of Physics, vol. 10, no. 3, 1987.

Pack, D. C. "On the Perturbation and Break Up of a High-Speed, Elongating Metal Jet." Journal of Applied Physics, vol. 63, no. 6, March 1988.

Pfeffer, G. "Determination Par Simulations Numeriques De L'etat et Des Lois De Fragmentation Des Jets De Charges Creuses." Proceedings of the Fifth International Symposium on Ballistics, Toulouse, France, April 1980.

Rayleigh, L. The Theory of Sound, 2nd. Ed., Reprinted by Dover in 1945, 1894.

Romero, L. A. "The Instability of Rapidly Stretching Plastic Jets." Journal of Applied Physics, vol. 65, no. 8, April 1989.

Rottenkolber, Ernst. "Zur Partikulation von HL-Stachein," MBB Internal Document AG 334, Schrobenhausen, Germany, 1989.

Shelton, R. D., and A. L. Arbuckle. "A Calculation of Particle Size Distributions in the Break-up of Shaped Charge Jets." Journal of Applied Physics, vol. 50, no. 10, October 1979.

Tomotika, S. "On the Instability of a Cylindrical Thread of a Viscous Liquid Surrounded by Another Viscous Fluid." Proceedings of the Royal Society, A 150, pp. 322–337, 1935.

Tomotika, S. "Breaking up of a Drop of Viscous Liquid Immersed in Another Viscous Fluid which is Extending at a Uniform Rate." Proceedings of the Royal Society, A 153, pp. 302–318, 1936.

Van Thiel, M., and J. Levatin. "Jet Formation Experiments and Computations With a Lagrange Code." Journal of Applied Physics, vol. 51, pp. 6107–6114, 1980.

Walsh, J. M. "Plastic Instability and Particulation in Stretching Metal Jets." Journal of Applied Physics, vol. 56, no. 7, October 1984.

Walters, W. P., and R. L. Summers. "The Particulation of a Shaped Charge Jet." Developments in Theoretical and Applied Mechanics, vol. 16. Edited by B. Antar, R. Engels, A. A. Prinaris, and T. H. Moulden, University of Tennessee Space Institute, Tullahoma, TN, 1992a.

Walters, W. P., and R. L. Summers. "The Velocity Difference Between Particulated Shaped Charge Jet Particles for Face-Centered-Cubic Liner Materials." ARL-TR-8, U.S. Army Research Laboratory, Aberdeen Proving Ground, MD, November 1992b.

Walters, W. P., and J. A. Zukas. Fundamentals of Shaped Charges, New York: John Wiley and Sons, 1989.

Zerilli, F., and R. Armstrong. "Dislocation-Mechanics-Based Constitutive Relations for Material Dynamics Calculations." Journal of Applied Physics, vol. 61, no. 5, pp. 1816–1825, March 1987.

No. of Copies	Organization
2	Administrator Defense Technical Info Center ATTN: DTIC-DDA Cameron Station Alexandria, VA 22304-6145
1	Commander U.S. Army Materiel Command ATTN: AMCAM 5001 Eisenhower Ave. Alexandria, VA 22333-0001
1	Director U.S. Army Research Laboratory ATTN: AMSRL-OP-CI-AD, Tech Publishing 2800 Powder Mill Rd. Adelphi, MD 20783-1145
1	Director U.S. Army Research Laboratory ATTN: AMSRL-OP-CI-AD, Records Management 2800 Powder Mill Rd. Adelphi, MD 20783-1145
2	Commander U.S. Army Armament Research, Development, and Engineering Center ATTN: SMCAR-IMI-I Picatinny Arsenal, NJ 07806-5000
2	Commander U.S. Army Armament Research, Development, and Engineering Center ATTN: SMCAR-TDC Picatinny Arsenal, NJ 07806-5000
1	Director Benet Weapons Laboratory U.S. Army Armament Research, Development, and Engineering Center ATTN: SMCAR-CCB-TL Watervliet, NY 12189-4050
(Unclass. only) 1	Commander U.S. Army Rock Island Arsenal ATTN: SMCRI-IMC-RT/Technical Library Rock Island, IL 61299-5000
1	Director U.S. Army Aviation Research and Technology Activity ATTN: SAVRT-R (Library) M/S 219-3 Ames Research Center Moffett Field, CA 94035-1000

No. of Copies	Organization
1	Commander U.S. Army Missile Command ATTN: AMSMI-RD-CS-R (DOC) Redstone Arsenal, AL 35898-5010
1	Commander U.S. Army Tank-Automotive Command ATTN: ASQNC-TAC-DIT (Technical Information Center) Warren, MI 48397-5000
1	Director U.S. Army TRADOC Analysis Command ATTN: ATRC-WSR White Sands Missile Range, NM 88002-5502
1	Commandant U.S. Army Field Artillery School ATTN: ATSF-CSI Ft. Sill, OK 73503-5000
(Class. only) 1	Commandant U.S. Army Infantry School ATTN: ATSH-CD (Security Mgr.) Fort Benning, GA 31905-5660
(Unclass. only) 1	Commandant U.S. Army Infantry School ATTN: ATSH-CD-CSO-OR Fort Benning, GA 31905-5660
1	WL/MNOI Eglin AFB, FL 32542-5000
	Aberdeen Proving Ground
2	Dir, USAMSAA ATTN: AMXSY-D AMXSY-MP, H. Cohen
1	Cdr, USATECOM ATTN: AMSTE-TC
1	Dir, ERDEC ATTN: SCBRD-RT
1	Cdr, CBDA ATTN: AMSCB-CI
1	Dir, USARL ATTN: AMSRL-SL-I
10	Dir, USARL ATTN: AMSRL-OP-CI-B (Tech Lib)

No. of Copies	Organization
5	Commander Naval Surface Warfare Center ATTN: Code DG-50, W. Reed, R10A E. Johnson W. Bullock F. Zerilli R. Garrett White Oak, MD 20910
3	Commander U.S. Army Armament Research, Development, and Engineering Center ATTN: SMCAR-AWE, J. Pearson J. Grant E. Baker Picatinny Arsenal, NJ 07806-5000
3	Director DARPA ATTN: J. Richardson T. Phillips T. Hafer 1400 Wilson Blvd. Arlington, VA 22209-2308
4	Commander U.S. Army Missile Command ATTN: AMSMI-RD-ST-WF, M. Schexnayder S. Cornelius S. Hill D. Lovelace Redstone Arsenal, AL 35898-5247
1	AFATL/DLJR ATTN: J. Foster Eglin AFB, 32542
1	WRDC/MTX ATTN: Mr. Lee Kennard Wright Patterson AFB, OH 45433-6533
1	U.S. Army Harry Diamond Laboratories ATTN: SLCHD-TA-SS, B. Christopherson 2800 Powder Mill Road Adelphi, MD 20783-1197

No. of Copies	Organization
1	Naval Ordnance Station ATTN: B. Barger-Tyo Code 6310C Indian Head, MD 20640-5000
9	Director Lawrence Livermore Laboratory ATTN: Technical Library Dr. J. Kury Dr. M. Van Thiel Dr. C. Cline Dr. D. Baum M. Murphy L. Haselman C. Simonson D. Lassila P.O. Box 808 Livermore, CA 94550
3	Battelle-Columbus Laboratories ATTN: Technical Library Dr. L. Vescilius Dr. B. Dale Trott 505 King Avenue Columbus, OH 43201
3	Sandia National Laboratories ATTN: Dr. M. Forrestal Dr. M. Vigil Dr. A. Robinson P.O. Box 5800 Albuquerque, NM 87185
9	University of California Los Alamos National Laboratory ATTN: Dr. J. Walsh Dr. R. Karpp Dr. C. Mautz L. Hull, M-8 J. Repa D. Fradkin L. Schwalbe M. Burkett Technical Library P.O. Box 1663 Los Alamos, NM 87545

No. of Copies	Organization
1	Southwest Research Institute ATTN: C. Anderson P.O. Drawer 28255 San Antonio, TX 78284
2	Battelle Edgewood Operations ATTN: R. Jameson S. Golaski 2113 Emmorton Park Road Suite 200 Edgewood, MD 21040
1	E.I. DuPont De Nemours & Company ATTN: B. Scott Chestnut Run - CR 702 Wilmington, DE 19898
1	Dyna East Corporation ATTN: P.C. Chou 3201 Arch Street Philadelphia, PA 19104-2588
1	Aerojet Electro Systems Company ATTN: Warhead Systems, Dr. J. Carleone 1100 W. Hollyvale St. P.O. Box 296 Azusa, CA 91702
2	Alliant Techsystems, Inc. Precision Armament Systems Group ATTN: G. Johnson J. Houlton 7225 Northland Drive Brooklyn Park, MN 55428
1	Nuclear Metals, Inc. ATTN: M. Waltz 2229 Main Street Concord, MA 01742

No. of Copies	Organization
4	Physics International ATTN: J. Coffenberry N. Collier R. Funston D. Tuerpe 2700 Merced St. P.O. Box 5010 San Leandro, CA 94577-0599
1	S-Cubed ATTN: Dr. R. Sedgwick P.O. Box 1620 La Jolla, CA 92038-1620
1	SRI International ATTN: Dr. L. Seaman 333 Ravenswood Avenue Menlo Park, CA 94025
2	University of Maryland College of Engineering ATTN: Dr. R. D. Dick Dr. R. Armstrong College Park, MD 20742
1	University of Alabama Department of Engineering Mechanics ATTN: Dr. S. E. Jones P.O. Box 870278 Tuscaloosa, AL 35487-0278
1	California Research and Technology, Inc. ATTN: Mark Majerus 50 Washington Road P.O. Box 2229 Princeton, NJ 08543
1	Olin Corporation Metals Research Laboratories ATTN: Frank Mandigo 91 Shelton Avenue New Haven, CT 06511

INTENTIONALLY LEFT BLANK.

USER EVALUATION SHEET/CHANGE OF ADDRESS

This Laboratory undertakes a continuing effort to improve the quality of the reports it publishes. Your comments/answers to the items/questions below will aid us in our efforts.

1. ARL Report Number ARL-TR-114 Date of Report April 1993

2. Date Report Received _____

3. Does this report satisfy a need? (Comment on purpose, related project, or other area of interest for which the report will be used.) _____

4. Specifically, how is the report being used? (Information source, design data, procedure, source of ideas, etc.) _____

5. Has the information in this report led to any quantitative savings as far as man-hours or dollars saved, operating costs avoided, or efficiencies achieved, etc? If so, please elaborate. _____

6. General Comments. What do you think should be changed to improve future reports? (Indicate changes to organization, technical content, format, etc.) _____

CURRENT ADDRESS

Organization

Name

Street or P.O. Box No.

City, State, Zip Code

7. If indicating a Change of Address or Address Correction, please provide the Current or Correct address above and the Old or Incorrect address below.

OLD ADDRESS

Organization

Name

Street or P.O. Box No.

City, State, Zip Code

(Remove this sheet, fold as indicated, tape closed, and mail.)
(DO NOT STAPLE)

DEPARTMENT OF THE ARMY

OFFICIAL BUSINESS

BUSINESS REPLY MAIL
FIRST CLASS PERMIT No 0001, APG, MD

Postage will be paid by addressee.

Director
U.S. Army Research Laboratory
ATTN: AMSRL-OP-CI-B (Tech Lib)
Aberdeen Proving Ground, MD 21005-5066

NO POSTAGE
NECESSARY
IF MAILED
IN THE
UNITED STATES